

UPPER LIMB PROJECT

Modeling of the upper limb

*Erik J.Dijkstra, BSc.
s0142395*

*This report is submitted in fulfillment of the work placement required for the degree of Master of
Science in Mechanical Engineering.*

*MSc. Biomechanical Engineering
Department of Engineering Technology
University of Twente*

October – December 2010

*Supervisor ORLAU
Dr. C. Stewart*

*Supervisor Keele University
Dr. A.D. Pandyan*

*Supervisor University of Twente
Dr. Ir. D. van de Belt*

Abstract

The upper limb is used in many activities of daily living(ADL), think about feeding and personal hygiene. Impairment can lead to inability or trouble in performing these ADL. Problems with the upper limb can arise due to impairments to the neurological or musculoskeletal system. The most common clinical condition where both systems are involved is spasticity. However the pathophysiology of spasticity is not fully understood. Current research is investigating the relationships between the impairment and human functioning by measuring the patients in ADL. These measurements are used to build a model of the upper limb, creating a way to further analyse and understand the relationships between impairment and human functioning.

From a systematic literature review, on upper limb movement analysis during reach and grasp movement, it became clear there are only a few studies done on upper limb kinetics. An additional search provided more kinetic data and guidelines on how to perform an upper limb movement analysis. These guidelines were used in a movement analysis of an eating movement where an eight camera Vicon system was used to collect kinematic data. The analysis protocol was kept in coherence with those found in previous studies.

With the data from the literature review, a basic model of the upper extremity was build to identify problems arising from modelling of the upper limb. The model build has seven degrees of freedom, three at the shoulder, two at the elbow and two at the wrist. Scapular movement was not taken in account due to its complexity. Every degree of freedom is represented by a revolute joint and the coordinate systems in the joints are described using the Denavit-Hartenberg convention. Matlab and Matlab Simulink were used to build an inverse and forward dynamics model.

During the simulations, crucial elements in forward dynamics are found to be the initial conditions, the time step, and the integration algorithm used. Also the order of the revolute joints turned out to influence the behaviour of the model especially for shoulder adduction movement. This is primarily related to the method for defining the coordinate frames in the revolute joints. Multi joint movement showed instability when one of the segments became an inverted pendulum.

When proceeding with modelling of the upper extremity, it is recommended to use a different method for programming the model because of restrictions within Matlab Simulink. A more thorough literature search on modelling should be performed to make mature choices in the method and algorithms to use. A feedback loop should be implemented in the forward dynamics to prevent unwanted behaviour.

Getting the skeletal model working means a step closer to the final goal of using an upper limb model to predict treatment outcome. However before this final goal is reached, muscle and neurological models should be implemented. Muscle and neurological models will help understand the relationships between impairment and human functioning as it can be used to simulate impaired human movement.

Table of Contents

Preface.....	3
1 Introduction	4
2 Anatomy of the upper limb.....	5
2.1 Bone structure	5
2.2 Joints.....	6
3 Clinical condition.....	7
3.1 What is spasticity.....	7
3.2 Pathophysiology of spasticity.....	7
3.3 Current assessment of spasticity.....	8
3.4 Discussion	8
4 Literature review	10
4.1 Search terms	10
4.2 Abstract screening	10
4.3 Full text selection	11
4.4 Data extraction	11
5 Upper limb movement analysis	14
5.1 Recording methods	14
5.2 Marker placement.....	14
5.3 Protocol for movement analysis	15
5.4 Vicon lab session.....	15
6 Modelling of the upper limb	16
6.1 The model	16
6.2 The InvArm function	18
6.3 Simulink SimMechanics	20
6.4 Hand calculation check.....	21
7 Results	23
7.1 Model behaviour.....	23
7.2 Initial conditions.....	25
7.3 New results.....	26
7.4 Sequence of revolute joints	28
7.5 Multi actuation	29
8 Discussion.....	31
8.1 Modelling of the upper limb	31

8.2	Discussion on the results.....	31
9	Future considerations	33
10	Reference list	34
I.	Protocol	36
II.	Matlab InvArm function.....	44
III.	Simulink block scheme	47
IV.	Model behaviour	48
V.	Sequence of revolute joints.....	55

Preface

A part of the master programme of Biomechanical Engineering at the University of Twente is an internship of at least ten weeks. This report describes the work I performed during my internship in the United Kingdom. It is part of a joint project between Keele University, at Keele, and ORLAU at Oswestry. ORLAU is a well respected research and development institute in Oswestry in England. The institute also offers clinical services for patients with mobility problems and provides education and training facilities for researchers and physiotherapists. Within Keele University I was stationed at the School of Health And Rehabilitation (SHAR), in the physiotherapy department, where I sat most of the days working on the project.

The main aim of the project was to create a basic model of the upper extremity to identify and address the problems arising from modelling. The first four weeks consisted of performing a literature review. For the remaining weeks I spend four days a week at Keele working on modelling of the upper limb. The other day of the week I had the privilege to take part in several clinics at ORLAU. Clinics ranged from clinical to pure technical clinics; Assessment of patient's mobility with and without the use of a gait lab, and reviewing and discussing clinical results of gait analysis of patients, to the calibration of the force plates in the gait lab. These clinics have been very educational and gave a good impression of the work field of a Bio-engineer.

I hereby would like to thank everybody who made this internship to a valuable experience, the warm welcome, the pleasant company of, and the support from the staff at Keele University and ORLAU. In particular I would like to thank Caroline Stewart and Anand Pandyan for their supervision and for arranging all the moments for me to gather new knowledge.

1 Introduction

Impairment can lead to disability and inability, or trouble, to perform activities of daily living (ADL). In order to help people improve their life when affected by impairment, there is the need of an understanding of the impairments and the impact they have on human functioning.

Measurements play an important role in understanding impairments as measurements quantify the parameters to describe the impairment. The measurements can be used to model the relationship between the impairment and human functioning, for example in ADL. Such a model will help get an understanding of the pathophysiology related to the impairment, comprehend the relationship and can be used to evaluate current rehabilitation methods used to treat the impairment.

The upper limb has a major contribution in the realization of ADL, think about feeding activities and activities of personal hygiene. Reduced ability to perform ADL where the upper limb has a crucial role therefore has a great impact on the quality of life. However, possibly due to the complexity of the upper limb, impairments of the upper limb have not been studied often. This is especially the case in neurological conditions where the failing of the neurological system (control component) leads to a failure of the skeletal system (mechanical component) which gradually worsens if the neural impairment is not resolved.

Within certain constraints the upper limb can be modelled. In this report a start is made on building a model of the upper limb to discover the challenging areas in modelling. Literature is reviewed to gain knowledge on analysis of upper limb function and a movement analysis was performed to collect data on upper limb movement during an activity of daily living. Although the work carried out is based on non-impaired subjects, the end aim is to apply the lessons learnt to develop solutions for people with disability.

This report can roughly be divided into five parts; introduction, literature, movement analysis, modelling, and evaluation.

- i. Chapter two and three, including this introduction, make the first part of the report. The two chapters discuss the anatomy of the upper limb, and the clinical conditions that are the main drive behind this study.
- ii. The literature review performed, describing a systematic approach to review literature is embedded in chapter four. Making it part two in the report.
- iii. Chapter five, the third part, discusses the movement analysis that took place for this project and will elaborate on some important issues regarding analysis reliability and inter study coherence.
- iv. The modelling is described in chapter six and seven. This comprises the model that is created for the purpose of analysing upper limb movements and dynamic behaviour, and the results from the forward model for different situations.
- v. The evaluation of the modelling and the report in general are discussed in chapter eight and nine where a discussion on the model and overall recommendations are given for future research on upper limb modelling.

2 Anatomy of the upper limb

This chapter gives an overview of the anatomy of the upper limb relevant for the purpose of this study. First the bone structures are described followed by the joints that form the connection between the bone structures.

2.1 Bone structure

The bones relevant in upper limb movement can be divided into four groups; the pectoral girdle, the upper arm, the forearm and the hand. Each of these groups and their bones will be discussed in respectively the same order. Figure 1 shows the bones in the upper extremity.

2.1.1 The pectoral girdle

The pectoral girdle consists of the clavicle anteriorly and the scapula posteriorly. It connects the upper limb to the axial skeleton and provides attachment sites for many of the muscles that control the movement of the arm.

The clavicle lies almost horizontally at the root of the neck and can easily be seen and/or palpated through the skin throughout its whole extent. Its most important functions are: to act as a brace to hold the scapula and arm laterally of the thorax, enabling the limb to swing clear of the trunk; and to transmit a part of the weight of the limb to the axial skeleton, in this way diminishing the muscular effort required for that purpose.

The scapula is a large, flattened, triangular bone. It lies on the posterolateral aspect of the chest wall, covering parts of the second to the seventh ribs.[2] Each scapula has three borders. The superior border is the shortest and sharpest border. The medial border lies parallel to the vertebral column. The thick lateral border abuts the armpit and ends superiorly in the glenoid cavity. This cavity articulates with the humerus, forming the shoulder joint.[3] The posterior surface of the scapula shows a prominent spine, easily felt through the skin, ending laterally in an enlarged, roughened triangular projection called the acromion. The acromion articulates with the clavicle, forming the acromioclavicular joint.

2.1.2 The upper arm

The humerus is the longest and largest bone of the upper limb. The proximal end consists of the head and the greater and lesser tubercles. The hemispherical head fits into the glenoid cavity and the tubercles are sites of attachment of the rotator cuff muscles. Immediately inferior to the head is the anatomical neck. The distal end of the humerus is expanded transversely and forms part of the elbow joint with the trochlea and capitulum. Anatomical landmarks are the medial and lateral epicondyle.

2.1.3 The forearm

The radius is one of the two bones in the forearm and lies on the lateral side. Upper and lower sides are both expanded. The proximal end consists of the head which is disk shaped and its surface is hollowed out to form a shallow cup for articulation with the capitulum of the humerus. The distal end is the widest part of the radius. Its lateral surface is slightly rough and projects downwards beyond the

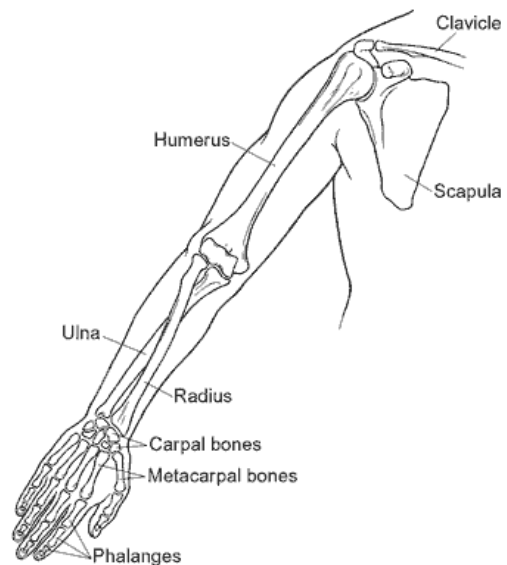


Figure 1: Bones upper extremity

rest of the bone to form the styloid process. This projection can be felt through the skin when the tendons concealing it are relaxed.

The ulna is the medial bone of the forearm and is parallel with the radius when the arm is in supine. The proximal end is thick, and hook like, the concavity of the hook directed forwards. The bone diminishes in size from its upper to its lower end, which bears a small, rounded enlargement termed the head of the ulna. At the proximal end of the ulna displays two substantial processes, the olecranon and coronoid, and two articular areas, termed the trochlear and radial notches. The trochlear notch articulates with the humerus and the radial notch with the radius. The distal end is slightly expanded and comprises the rounded head and the styloid process.

2.1.4 The hand

The carpus are the eight short bones in the wrist, which are arranged in a proximal and a distal row, each containing four bones.

2.2 Joints

The three joints that will be discussed are the glenohumeral joint, the elbow, and wrist joint. The glenohumeral joint, also known as shoulder joint, is formed by the humeral head and the glenoid cavity of the scapula. In general it has three rotational degrees of freedom, flexion and extension, ab- and adduction, and in- and external rotation. The ligaments and muscles keep the humeral head in place ideally constraining translational movement. A mechanical representation of this joint is a ball and socket joint as can be seen in Figure 2.

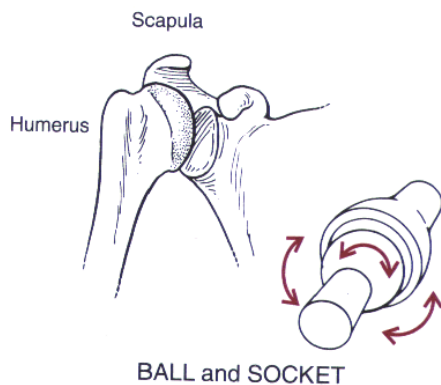


Figure 2: Shoulder joint

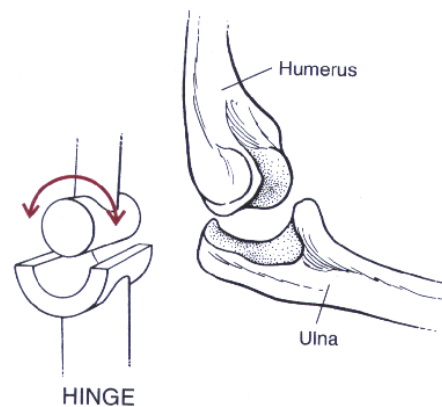


Figure 3: Elbow joint

The elbow joint can be regarded as a hinge joint, see Figure 3, allowing flexion and extension in the elbow. The movement freedom in all other directions can be neglected as they are suppressed by ligaments, muscles and the bony structures.

Slightly more distal from the elbow joint, a second degree of freedom, pronation and supination of the forearm originates. A mechanical equivalent for this type of joint is a pivot joint, shown in Figure 4.

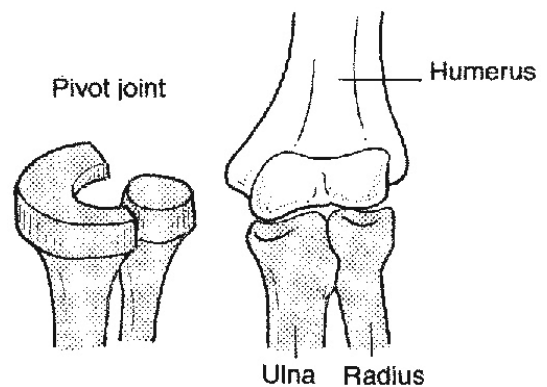


Figure 4: Forearm rotational joint

Finally wrist flexion and extension and wrist deviation are both occurring at the distal end of the forearm, where ulna and radius are articulating with the carpal bones.

3 Clinical condition

Upper limb problems can arise due to impairments in the musculoskeletal system, or the neurological system. There are however clinical conditions where both systems are affected. The most common clinical condition where both systems are involved is spasticity. Spasticity is an impairment arising from a problem in the neurological system. This can lead to problems interfering with the performance of the musculoskeletal system, and in certain cases lead to changes in the biomechanical properties of the mechanical system. This chapter will elaborate further on what spasticity is, its pathophysiology, and current methods of assessing spasticity.

3.1 What is spasticity

Spasticity is a motor disorder associated with upper motor neurone lesions. [4] The disorders in which spasticity is a common finding are [5];

- Multiple sclerosis (MS); A disorder where the myelin sheets around the nerves are affected, resulting in poor transmission of signals through the nerves.
- Stroke; Ischemic or hemorrhagic stroke can cause severe damage to the area of the brain affected. Either caused by a short on oxygen and nutrients in the brain cells or toxicity due to rupture of a blood vessel. [6]
- Cerebral palsy (CP); The term cerebral palsy may refer to any one of a number of neurological disorders that appear in infancy or early childhood. It permanently affects body movement and muscle coordination but is not progressive. In some cases of cerebral palsy, the cerebral motor cortex hasn't developed normally during fetal growth. In others, the damage is a result of injury to the brain either before, during, or after birth. [7]
- Spinal cord injury (SCI); damage to the spinal cord can occur due to a traumatic blow to the spinal column or other disorders, like MS or stroke. It can be classified as complete or incomplete depending on the ability of the spinal cord to convey messages from and to the brain. [8]
- Head injuries; Refers to trauma to the head. This may or may not include damage to the brain. Traumatic brain injury belongs to this group. Common causes are traffic and domestic accidents, falls, and assaults.

3.1.1 Definition

There are many different definitions for spasticity, but the most accepted seems to be Lance's definition. [4]

Spasticity is a motor disorder that is characterised by a velocity dependent increase in the tonic stretch reflex with exaggerated tendon reflexes, resulting from the hyper-excitability of the stretch reflex, as one component of the upper motor neurone syndrome.

More recently, the definition of Lance was found to narrow, it is suggested it should be widened to;

Disordered sensori-motor control, resulting from an upper motor neuron lesion, presenting as intermittent or sustained involuntary activation of muscles.

The widened definition seems to be more in line with the current understanding of pathophysiology and clinical practice.[9]

3.2 Pathophysiology of spasticity

The pathophysiology of spasticity is not clearly understood. However there are several theories proposed to explain the abnormal reflex responses and muscle contractions but first it should be made

clear that spasticity is not always considered to be a problem. Spasticity is only considered a problem as it interferes with the ability to perform a task. If spasticity does not affect the individual's ability to perform tasks, it is often not treated.

The mechanisms proposed to explain spasticity all involve the neurological system. The neurological system is the controller component of the human. It can be described in more engineering terms as a structure containing many positive, but also negative, feedback loops. Muscle spindles, Golgi tendon organs, and other sensors are the organelles providing the feedback to the controller.[3] Most of the feedback is positive feedback however there are also negative feedback loops like the negative feedback of the 1b afferents from the Golgi tendon organs. Other controller input are the signals originating from the different spinal tracts.[10]

An important mechanism involved in spasticity is the inhibitory synaptic input. In mechanical systems one can turn off certain actuator signals. However this is not possible in the human system, where active negative activation of the inhibitory nerves is needed to inhibit the actuator signals. The inhibitory pathways can therefore be considered as negative feedback loops, having the ability to reduce the signal input to the muscles.[10] Some neurological injuries turn off these inhibitory pathways. The loss of this active inhibition is the most probable reason for seeing the signs of spasticity.

3.3 Current assessment of spasticity

Different methods can be used to measure spasticity. Malhotra et al.[9] investigated the different measurement methods in literature and the methods found can roughly be divided in three groups; EMG, biomechanical, and scales. Surface EMG can be used to quantify the muscle response to stretch by using the H-reflex or F-reflex response. Biomechanical measures often use stiffness during a controlled motorized perturbation as an indirect measure of spasticity. However the most applied assessment method in clinical practice will be the use of scales. Tardieu scale, Ashworth scale, and Modified Ashworth scale are just a few examples. The scales do not require any appliances and can be performed by the physiotherapist alone. The physiotherapist moves the limb through its range of motion at different velocities, sensing for resistance and the occurrence of a 'catch' during movement.

3.4 Discussion

With the pathophysiology of spasticity not fully understood, it is difficult to give an unambiguous definition. Therefore measurements are used to get a better understanding of the impairment. The use of biomechanical and EMG methods in measuring spasticity both involve expensive equipment and need specialists to operate the systems. It is therefore less applied in clinical practice and currently most used in research settings.

The scales that are widely used in clinical practice have one major drawback. The measurement is performed by a human and therefore unreliable. Many parameters like temperature, cooperation of the patient, state of muscles of the physiotherapist performing the measurement, will influence the accuracy with which the physiotherapist can determine the resistance in a limb. The results from a patient assessed by two physiotherapists, both performing the same test, may not be the same. But the most inaccurate measure will be the detection of the catch and relating it to a certain angular position, as used in the Tardieu Scale. When the catch happens the sensory information has to travel to the brain before the physiotherapist actually senses it and in that time the limb has been moved further and thus the angle associated with the catch is overestimated.

Spasticity is affecting both the musculoskeletal and neurological system. However the neurologically side of spasticity is not fully understood. To model the neurological system it is necessary to have a musculoskeletal model first. Then the neurological model can be build, as a package, on top of the

musculoskeletal model. Thus there is the need for a musculoskeletal model of the upper limb and therefore also information on upper limb analysis and upper limb properties. Next chapter discusses the literature review performed to retrieve the necessary information.

4 Literature review

There are several stages in a literature review. First the search terms are determined, based on the information needed. Next a search is performed with these search terms in the appropriate, depending on subject, search engines. An example is the use of PubMed for medical journals. The resulting articles will then be screened on whether they will provide the information necessary, by reading the abstracts. Next step is to find the full text of the articles left, and read them. Even though some articles may look promising from the abstract, it does not always correlate with what the full text comprises. In the end a selection of articles has been found useful and data can be extracted and used in the research project.

The literature review described in this chapter does not start at the first stage. The search of the articles, matching the search terms, has been performed by associates. The process starts at the screening of the abstracts. Nevertheless, the following paragraphs will give a description of all the steps in the literature review for this project

4.1 Search terms

As mentioned above, the first stages of literature research are performed by associates. However to get an overview of the process, a short summary will be given on the search process.

When defining the search terms it is important to look at the information required for the research. For the project it was to find out what is known in the area of upper limb kinematics and kinetics. In general three groups of search terms are used. Search terms related to the structure in this case the upper extremity. Terms linked to what has been measured and terms involving the movements performed.

- Structure; upper extremity, upper limb, wrist, elbow, shoulder, finger, arm, hand, muscle
- Movement; grip, grasp, reach
- Measurement; kinematic, displacement, velocity, acceleration, movement, kinetic, torque, moment, force,

All the search terms are used in different combinations with operator terms like AND and OR to retrieve the best results. The search terms can be used as title words or general search terms. The search has been performed in the MEDLINE database. Also several medical headlines are used to refine the search. After deleting the inappropriate titles and duplicates, this resulted in a selection of three hundred articles to be screened.

4.2 Abstract screening

With the articles resulting from the search the next stage in the process can begin. For the current study, the abstracts are screened using several criteria. Each of them is mentioned with a short explanation.

- English language: The article should be written in English.
- Peer reviewed: Has the article been checked on validity?
- Subject age ≥ 18 : Are the subjects used in experiments 18 years or older?
- Human subject: Is the subject used human?
- Experiment/review: Does the article comprise an experiment or a review?
- Alive and well: The subjects must be alive and well. Cadaver studies are not to be included.
- Non-impaired control: In case of impaired subjects are there non-impaired controls?

- Reach to grasp, grip or point: Does the article describe any of the mentioned movements?
- Shoulder and elbow movement: Is shoulder and elbow movement investigated?
- Excluding trunk compensation: Is the trunk movement restrained or compensated for?
- Exo-skeletally unconstrained movement: Are the movements made natural movements without external constraints?
- Measurement of timing kinematics/kinetics: Are there measurements taken regarding timing, kinematics and/or kinetics? Think of trajectories, moments/forces, and joint angles.

For each of these criteria a point could be rewarded if the question is answered positively. The total sum of points gave an idea of the relevance of the article concerned for this research. Articles with ten or eleven points are most likely to be relevant however can be placed in a different group. For instance if there are no healthy or human subjects, the article will be rejected, even if it scores on all other criteria.

Out of the three hundred article abstracts, 112 seemed relevant, 50 were to be considered, and the remaining 138 articles could be rejected.

4.3 Full text selection

Normally, before starting a full text selection process, if there are that many relevant articles remaining after an abstract screening, a discussion will take place between the reviewers. The outcome of such a discussion might result in a reduced number of relevant articles, reducing the workload. In this case this discussion has not taken place. Therefore all 112 articles were listed for a full text review.

With this many articles it is wise to selectively read certain sections of the articles. Most articles use a general format where first an introduction is given. After the introduction methods are discussed, giving information about the participants used in an experiment, experimental set-up, and methods used for data analysis. After the description of the methods often the results will be presented, either in words or in graphs to end with a discussion and a conclusion.

In search for useful data on kinetics and kinematics of the shoulder and elbow joint during reach to grasp movements, the following approach was taken; At first instance only the methods and results paragraphs were read. If these had interesting content, the article was read as a whole. Articles not using the structured format were read entirely.

This stage of the literature review process resulted in only three useful articles. Many articles did describe the timing aspects of the movements but when it came to kinetic, joint angle or trajectory data only wrist or fingers were reported.

4.4 Data extraction

The final stage in a literature review is the data extraction. The data in the final selection of articles will be collected and processed for the purpose of the study.

For this project the data of interest is any data on the kinematics and dynamics of the shoulder and the elbow during reach movements or activities of daily living. Besides that it is useful to know how many healthy subjects are represented in the data and what type of measuring method is used.

Jacquier-Bret et al.[11] performed a preliminary study where one C6 quadriplegic patient and control were analysed during a reach to grasp task. Apart from elevation, results show the patient's joint angles are six to seventy percent of angles used by the control. Muscle activity was 1.14 to 5.85 times higher for patient compared to control, concluding that the patient is using kinematic compensatory

strategies. The C6 patient compensated a task change primarily in the elbow compared to the all joint recruitment in the control subject.

Gréa et al.[12] observed nine subjects performing a grasp movement to a cylinder that was perturbed. Results show the final arm position and wrist trajectory showing that final posture is planned in advance and used as control variable in the central nervous system.

Marotta et al.[13] performed two experiments. 14 subjects were to reach to a block of which the orientation could be perturbed. The results comprise three dimensional trajectories of the arm and torsion of the upper arm as function of the lower arm torsion with respect to the upper arm. Data show that a linear relation exists between upper and lower arm torsion, making the components of the arm rotate in coordination with one another. Arm rotation only accommodated for about half of the re-orientation required to align grasp with the block. The formation of hand and fingers must therefore account for a large portion of the required torsional rotation. These observations show that the entire arm-hand system contributes to grasp orientation.

4.4.1 Additional articles

The three articles found through the literature search did not provide all the data required, therefore another simple search of a known author is performed to get additional articles.

The author used for the search is Murray as he is known to have worked in the area of upper limb kinetics. An article written by Murray and Johnson[14] is used to find more articles. They performed a study on the external forces and moments at the shoulder and elbow while subjects performed everyday tasks. From this article four additional studies, retrieved from the reference list, found to provide useful information.

Murray and Johnson[14] studied ten subjects to establish a database of upper limb kinematics and kinetics. Data on ranges of motion and external forces and moments were collected. Greatest range of motion (111.9°) and maximum moment (14.3 Nm) at the shoulder occurred during reach and lift tasks. For elbow flexion reaching the back produced the greatest elbow flexion (164.8°) but greatest elbow flexion moment (5.8 Nm) occurred in a lifting task.

Kontaxis et al.[15] proposed a framework for the definition of standardized protocols for measuring upper limb kinematics. Summarizing essential steps in a motion analysis protocol, basic recommendations are formulated and problems identified.

Buckley et al.[16] gave a review of the current knowledge on dynamics of the upper limb during ADL. Discussing the few published results on upper limb kinematics, they found differences in methods and joint axes definitions. These differences make it difficult to compare the results. It is also noticed there is a lack of data on limb segment orientations, velocities and accelerations. Available results suggest that current rehabilitation manipulators and orthoses move at far lower speeds than the healthy human arm.

Morrey et al.[17] studied thirty-three subjects on elbow movement during fifteen ADL. Functional arc of motion of elbow flexion was found to be 100 degrees, 30 to 130 degrees. Tests could be accomplished with 50 degrees of pronation and 55 degrees of supination. Rotation of the forearm is difficult to measure clinically as the zero position can only be approximated and carpus rotation cannot be excluded.

Barker et al.[18] used flexible electrogoniometers to measure shoulder, elbow and wrist angular motion in three dimensions during simulated ADL on seven healthy subjects. Motions produced by muscles controlling multiple joints were plotted against each other to study joint co-ordination. Two parameters were derived to mathematically describe the shape and orientation of the angle-angle

graphs. Slope, to represent the relative magnitude of changes in the joint angles used, and movement area quotient to say something about the timing difference between the relative motion of the two joint variables.

Besides these additional five articles, another source of information was the thesis submitted by Murray in 1999, to obtain his PhD degree[19]. This thesis reported on the determination of upper limb kinematics and dynamics during everyday tasks, providing information regarding length, mass, and inertia properties of the segments of the upper limb. Apart from the body parameters, a model of the upper limb was made using the robotics toolbox [20]in Matlab.

4.5 Discussion

The search result showed a lot of articles concerning the hand and finger kinematics without mentioning the elbow and shoulder. Since shoulder and elbow joint kinematics and kinetics is the area of interest most articles did not come through the screening and an additional search was needed.

The majority of the relevant studies found, give information on the kinematics of the upper limb during ADL. Joint movement is given in mean angles, maximum angles or angular range of motion. Due to the difference in the experimental protocols used it is difficult to compare these quantitative measurements. Essential issues to take in account for comparison are therefore coordinate systems and zero definitions. This emphasises the importance of the coordinate frames and also the protocols to use when building a model or doing movement analyses.

The literature search provided useful information, if not useful now it will be applicable when the modelling has reached a more mature state. Joint co-ordination and muscle activities for example can be used when a muscle model is implemented. However when keeping in mind the goal of building a basic model of the upper limb, some essential issues have not been elaborated in the articles. The studies encountered till now all deal with the kinematics of the upper limb, some also using inverse dynamics methods to derive the forces and moments acting on the limb segments.

Modelling methods is not elaborated on and the main emphasis is on the kinematics and, if investigated, kinetics of the upper limb. Murray and Johnson [14],used a recursive Newton –Euler technique and the Matlab Robotics toolbox but did not elaborate on why they used this method. Via the author search on Murray the segment properties of the upper limb were found, proving to be good validated data but forward dynamics studies, where primarily algorithms and modelling methods are discussed, are still missing. A new search for articles is recommended to obtain the more engineering and mathematical topics behind modelling and movement analysis of the upper extremity.

5 Upper limb movement analysis

For long the motion of the upper limb has been observed and admired, but a systematic study requires the application of appropriate measurement techniques.[18] Recent developments in the area of information technology enabled most laboratories to have access to sophisticated motion analysis equipment.[16] This chapter comprises an overview of the recording methods used in the literature and will discuss several important issues with respect to the marker recording methods. Also the standardization of protocols for measuring upper extremity kinematics will be highlighted while describing a protocol for the kinematics data collection performed.

5.1 Recording methods

For a movement analysis, different systems can be used. Morrey et al.[17] used goniometers, where an orthosis is equipped with goniometers to measure the joint angles. Although the accuracy of such a system is sufficient, it can be said that the use of an orthosis limits the subject to make a natural movement. Therefore more emphasis is placed on video based systems for the tracking of movements.

Mainly two different forms of video tracking are regularly encountered in literature. Systems like OPTOTRAK used by Marotta et al.[13], and SELSPOT used in research conducted by Gréa et al.[12], use infra-red emitting diodes placed on the subject. An infra-red sensitive camera system detects the diodes and records their movement. These systems are similar to a Vicon system, where the markers placed on the subject are small spheres covered in reflective material. This difference also shows the disadvantage of the IRED systems compared to a reflective marker system. The power supply necessary for the IRED's requires power cables to be attached along the body of the subject, inflicting with the wish to analyse in a situation as natural as possible.

Even though Vicon is the most well known system using reflective markers there are also other software packages that can be used with reflective markers. Murray and Johnson used APAS software to process the data collected of tasks associated with daily living using four video cameras.[14] However there are also many researchers writing their own programme to process the captured data from the cameras.

5.2 Marker placement

With regard to marker placement certain aspects should be kept in mind. The positioning of the markers and the positioning of the subject to be analysed are crucial. On each body segment, at least three markers must be visible at all times to define its position and orientation.[14] The accuracy of the measurements will be influenced by marker movement relative to both underlying skeleton and other markers.

As the placement of the markers is important for the cameras to be able to spot the spheres, it is also crucial as the marker positions are used to build the model within the software. A misplaced marker can result in a biased joint angle and, if not noticed, cause a wrong interpretation of the results.

In practice it might occur that one of the markers falls of during the recording of a movement. To quickly replace the marker without again having to palpate the subject, one can mark the skin surrounding the sticky tape of the marker after placing the markers to define its position on the limb.

5.3 Protocol for movement analysis

In order to be able to compare the results from different studies it is required that the protocols used have no conceptual or practical difference. Kontaxis et al.[15] proposed a framework to standardize protocols for measuring upper extremity kinematics. This framework has been used as a guideline for the movement analysis performed in this study. The protocol used in the movement analysis can be found in appendix I. A short summary of the Vicon lab session is given below.

5.4 Vicon lab session

A kinematic data collection of an upper limb movement was conducted in order to get acquainted with movement recording with the use of a Vicon system.

5.4.1 Method

The movement recording took place in the Vicon lab of Keele University. Kinematic data was collected using an eight camera Vicon system. Data was collected at a frequency of 100 Hz. The movement recorded was an eating movement where the subject brought the hand to the mouth and back again to the initial position. The collected data was processed off-line using the Vicon software.

Participants; For this movement analysis experiment only one subject was recruited, in the shape of the researcher himself. The subject has no history of impairment to the upper limb.

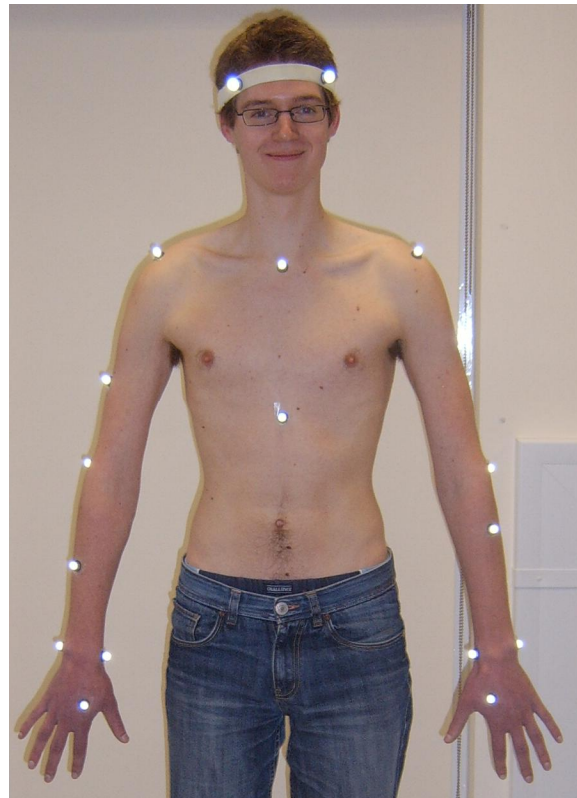


Figure 5: Subject with markers positioned on upper body

For marker positioning Vicon documents on Plug in Gait Marker placement were used.[21] The marker positions on the subject can be seen in Figure 5. A more detailed description of the marker positioning, movement made, and data processing can be read in the protocol in appendix I.

5.4.2 Results

From the data collected during the eating movement, angular positions in the joints have been derived. The Vicon software could also provide the angular velocity and acceleration. The kinetics of the movement could not be calculated by the Vicon software, as there was no kinetic data collected.

6 Modelling of the upper limb

This chapter discusses the modelling of the upper limb. First the different segments and their interrelation are described with the use of Denavit-Hartenberg parameters. Next the kinetic and kinematic equations are written for the recursive Newton-Euler algorithm. To check the model it has been verified with a hand calculation. Finally the implementation of the inverse and forward model in Simulink is presented.

6.1 The model

The human arm model can be represented by a kinematic chain model. A kinematic chain model describes the relative positions between links of the arm and gives the axis of rotation for all the joints. Murray[19] used a kinematic chain model to evaluate the data from a movement analysis. This modelling approach has also been taken by Naaij[22] who studied the working space representation of the human arm. The arm model created in this study is based on the work of Murray.[19]

The model has seven degrees of freedom, corresponding to the seven axes of rotation. Three axes of rotation in the shoulder for flexion and extension, abduction and adduction, and internal and external rotation of the upper arm. Two axes of rotation in the elbow, one for flexion and extension and one for pronation and supination of the forearm. Another two axes at the wrist to accommodate flexion, extension and radial/ulnar deviation of the hand. A graphical representation of the model can be seen in Figure 6. The coordinate frames at each of the joints are defined using the Denavit-Hartenberg convention. An example of the use of the D-H convention is given in the next paragraph.

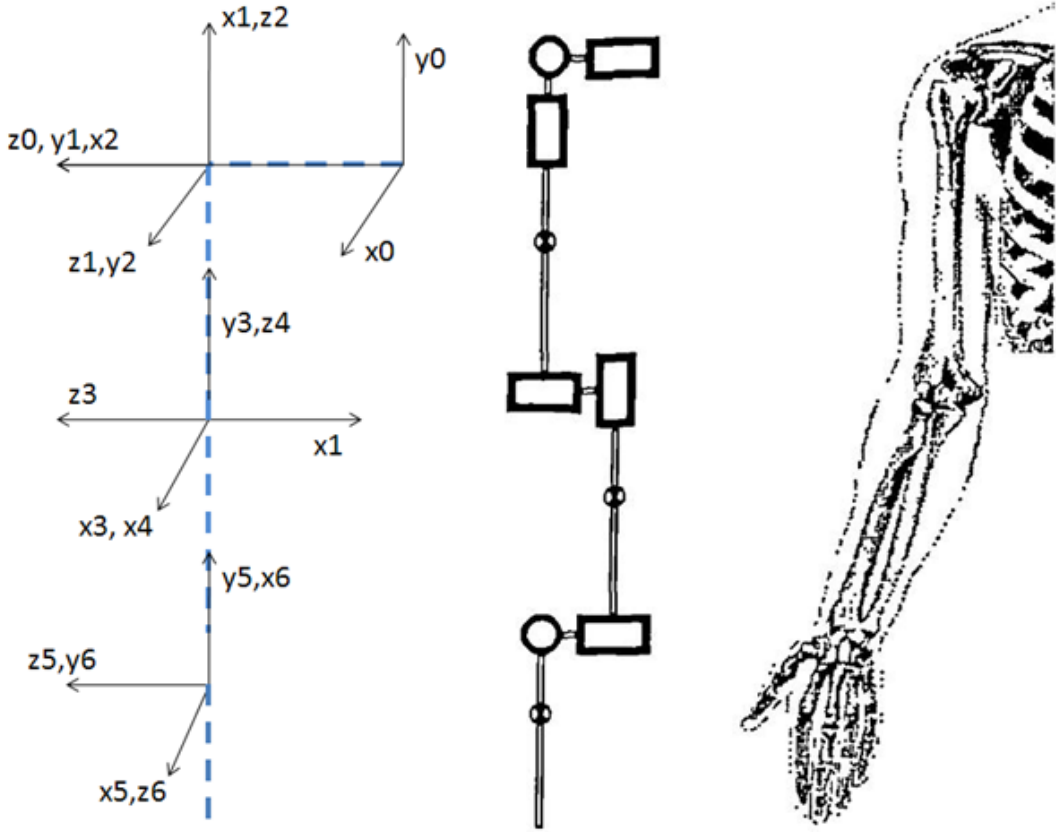


Figure 6: Model arm representations with left; coordinate frames, middle; technical representation, right; human arm.

6.1.1 Denavit-Hartenberg convention

The Denavit-Hartenberg convention is often used for selecting reference frames in robotic applications. Since the human arm can be compared to a robotic arm, this convention is also widely used in biomechanical studies. With two rotation and two translation parameters the minimal representation of one frame to another is obtained. Four parameters, from now on referred to as D-H parameters, are the parameters which describe the relation between two consecutive coordinate frames.

To get an idea of how this convention works an example is taken to explain the selection of the frames and the four parameters. The structure to explain the D-H convention can be seen.[1]

For the first joint, define the z-axis along the axis of rotation, or along the axis of translation in case of a prismatic joint. The x-axis of the base frame can be chosen freely after which the y-axis follows from the right hand rule to complete the coordinate frame. For the next joint again the z-axis is along the axis of rotation of the revolute joint. The x-axis is along the common normal of both z-axes, also the shortest distance between the two, and therefore the origin does not have to be in the centre of the joint. The D-H parameters only concern the motion of the links and not the physical placement of components.

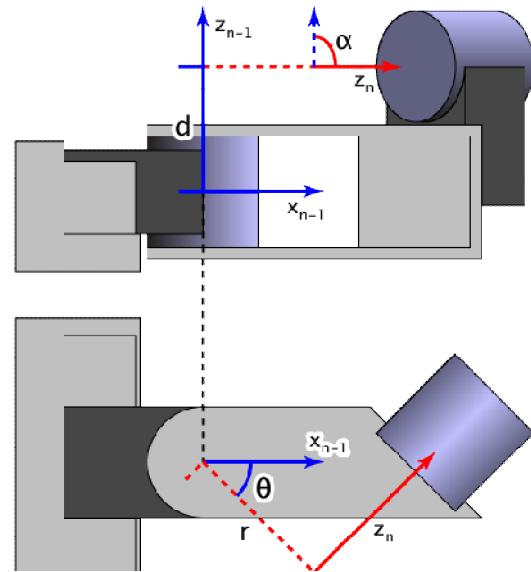


Figure 7: Denavit-Hartenberg example[1]

The parameter d is the depth along the previous joint's z-axis from the origin to the common normal. Angle α rotates about the previous z-axis from the previous x to the new x-axis. r is the length of the common normal itself. Originally this parameter is named a but since there is an a to confuse it with r is chosen since it is also the radius of rotation about the previous z-axis. The fourth parameter, θ , is the angle about the new x-axis from the previous z-axis to the current z-axis. By using this convention only four parameters are necessary to describe a frame with respect to its previous frame. [1]

6.1.2 Parameters

All the joints in the model are connected to each other with bodies, also described as links. As can be seen in the technical representation of the arm in Figure 6, three of the links have a mass. These three links represent the segments of the upper limb. Starting from the shoulder; upper arm, forearm and hand respectively.

In case of a robot it would be easy to determine the segment properties as you can disassemble the robot to measure every segment separately. The properties of the segments of the human upper limb on the other hand are not that easily obtained. Because the properties of the segments of the upper limb are different for every individual and the measurements impossible or cumbersome to perform on living subjects, it is necessary to estimate the parameters. Murray also addressed this problem and stated that for the modelling of the human upper arm for a quantitative biomechanical analysis, it is necessary to estimate certain characteristics of the body segments considered.[19] Body segment characteristics are the dimensions of the bodies, its masses, centre of masses and their moments of inertia.

The segment parameters used in the model of Murray[19] are also applied for this model. With the segment lengths known the D-H parameters could be determined. An overview of all the parameters, used to describe the upper limb model, is presented in Table 1.

	D-H parameters				M	Centre of mass locations			Moments of inertia		
	θ	d	r	α		Cm_x	Cm_y	Cm_z	I_{xx}	I_{yy}	I_{zz}
Link 0	0	-lc	0	0	0	0	0	0	0	0	0
Link 1	$\theta_1 + \frac{\pi}{2}$	0	0	$\frac{\pi}{2}$	0	0	0	0	0	0	0
Link 2	$\theta_2 + \frac{\pi}{2}$	0	0	$\frac{\pi}{2}$	0	0	0	0	0	0	0
Link 3	$\theta_3 + \frac{\pi}{2}$	-lua	0	$\frac{\pi}{2}$	Mua	0	0	-cmua	T	A	L
Link 4	θ_4	0	0	$-\frac{\pi}{2}$	0	0	0	0	0	0	0
Link 5	θ_5	-lfa	0	$\frac{\pi}{2}$	Mfa	0	0	-cmfa	A	T	L
Link 6	$\theta_6 + \frac{\pi}{2}$	0	0	$\frac{\pi}{2}$	0	0	0	0	0	0	0
Link 7	θ_7	0	-lh	$\frac{\pi}{2}$	Mh	cmh	0	0	L	A	T

Table 1: Model parameters

With:

- Lc, the length of the clavicle, the distance from sternum to the shoulder.
- Lua, the length of the upper arm.
- Lfa, the length of the forearm.
- Lh, the length of the hand.
- Mua, the mass of the upper arm.
- Mfa, the mass of the forearm
- Mh, the mass of the hand
- Cmua, the centre of mass location of the upper arm along the longitudinal axis.
- Cmfa, the centre of mass location of the forearm along the longitudinal axis.
- Cmh, the centre of mass location of the hand along the longitudinal axis.
- L, A and T stand for longitudinal, anteroposterior and transverse respectively. Determining which radius of gyration to use in the calculation of the moment of inertia.
- θ_i , the angle of the i^{th} revolute joint.

With the kinematic chain model and the dynamic parameters an inverse dynamics model can be constructed. An inverse dynamics arm model allows the calculation of the torques/moments necessary at the joints to produce a certain movement given the accelerations and all other parameter values each instant of time.

6.2 The InvArm function

For the evaluation of the inverse dynamics of the arm model, the InvArm function is developed. This function is a Newton-Euler analysis of free-body motion based on the model of Swartz [23]. Swartz

described a mathematical model to model the movement of a robot manipulator and used it to simulate and control a real robotic arm. The inverse dynamics model comprises five steps. These five mathematical steps with their equations are given in the next paragraph.

6.2.1 Kinematics

The first step is the calculation of the velocities and accelerations of each link. For each link there are two forms of velocities and accelerations considered, linear and angular. This gives four equations, see eq. (1) to (4), which can be solved iteratively from link one to link eight to find the angular and linear accelerations and velocities of each of the links of the arm. Here A_{i+1}^i is the rotation matrix from link $i + 1$ to link i . The base link only has linear acceleration equal to the gravitational acceleration in the direction of gravity. The angular acceleration and both forms of velocities of the base link are assumed to be zero.

$$\omega_{i+1} = A_{i+1}^i(\omega_i + Z_0 \dot{\theta}_{i+1}) \quad (1)$$

$$\dot{\omega}_{i+1} = A_{i+1}^i(\dot{\omega}_i + Z_0 \ddot{\theta}_{i+1} + \omega_i \times Z_0 \dot{\theta}_{i+1}) \quad (2)$$

$$v_{i+1} = \omega_{i+1} \times p_{i+1} + A_{i+1}^i v_i \quad (3)$$

$$\dot{v}_{i+1} = \dot{\omega}_{i+1} \times p_{i+1} + \omega_{i+1} \times (\omega_{i+1} \times p_{i+1}) + A_{i+1}^i \dot{v}_i \quad (4)$$

The second step is the calculation of the linear acceleration of the centre of mass for each link. This equation is similar to the linear acceleration of the links but then with the vector s_i pointing to the centre of mass from the link's origin instead of the vector p_i which is the vector pointing from the link $i-1$ to the link i coordinate system.

$$\dot{v}_{cm_i} = \dot{\omega}_i \times s_i + \omega_i \times (\omega_i \times s_i) + \dot{v}_i \quad (5)$$

With these equations the kinematic characteristics of the upper arm are described. In order to calculate the kinetics of the arm the additional three steps should be performed.

6.2.2 Kinetics

The calculation of the net forces and moments is the third step in the process of building the model. Since the accelerations of the centres of mass are known from the previous equations, Newton's law and its analog to rotational dynamics can be used to compute the net forces and moments acting on the centre of mass of each link.

$$F_i = m_i \dot{v}_{cm_i} \quad (6)$$

$$N_i = J_i \dot{\omega}_i + \omega_i \times (J_i \omega_i) \quad (7)$$

The angular analog is a form of Euler's equation of motion for a rigid body. With J_i , the moment of inertia around the link centre of mass.

The fourth step is the calculation of the local forces and moments acting on each link. As each link is connected to two other links, except for base and hand, forces from the two links are exerted on that link. The net force on the link is the sum of these two forces. The local moment of each link has four components. Two moments are from the interaction with the adjacent links like with the force. The moment caused by the local force acting on the link at a distance away from the origin. And last the moment caused by the net force acting on the centre of mass of the link.

$$f_i = A_i^{i+1} f_{i+1} + F_i \quad (8)$$

$$n_i = A_i^{i+1} n_{i+1} + p_i \times (A_i^{i+1} f_{i+1}) + s_i \times F_i + N_i \quad (9)$$

These four equations, equation (6) to (9), can again be solved iteratively, this time from the most distal link to the base link. After solving the kinematics and the net and local forces and moments the final step can be performed. This final step is the computing of the torques required for a joint to compensate for the local moment and friction.

$$\tau_i = n_i \cdot (A_i^{i-1} Z_0) + b_i \dot{\theta}_i \quad (10)$$

The above mentioned equations are implemented in a Matlab function that evaluates the equations one through ten. This function produces the torques given the angular position, velocity and accelerations of each link. The Matlab code of the InvArm function can be found in Appendix II.

6.3 Simulink SimMechanics

The model of the arm is also implemented in Matlab with the use of SimMechanics, a toolbox within the Simulink package. With this toolbox the revolute joints and the bodies are building blocks. The blocks have an input and output and parameters can be given to each block. For the joints this is the axis of rotation and for the bodies it is the mass, the inertial tensor, the centre of mass, body dimensions, and coordinate system on each end of the body. A piece of the schedule can be seen in Figure 8. Where the orange blocks are the joint actuators and the IC blocks enable one to set the initial angle and angular velocity.

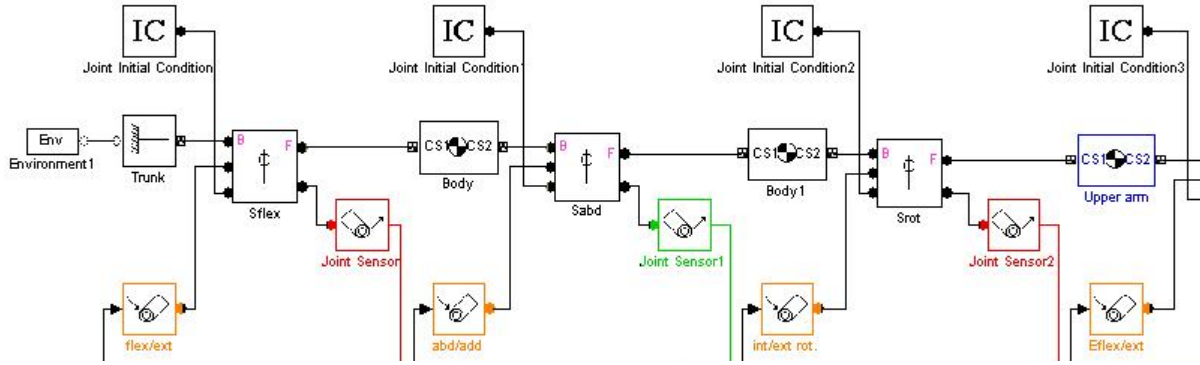


Figure 8: Simulink block scheme

The relation between the coordinate systems can be described using different conventions. The Euler-angle convention is used as it is the most straightforward in producing the same coordinate systems used in the InvArm function. Other options would be the use of quaternions where there is a rotation about a defined vector, or a 3x3 orthogonal rotation matrix. The full block scheme can be found in Appendix III. Both the programmed and the SimMechanics model are checked with a hand calculation as discussed in the next section.

6.4 Hand calculation check

To check the inverse dynamics models a hand calculation was made to verify the model output. As the entire system of rigid bodies is too complex for a hand calculation, only the most distal segment was given an input. This reduces the hand calculation to solving the relatively simple equation of a single pendulum (Figure 9). The Lagrange equations for this calculation are shown below.

The term with the moment of inertia(I) in equation (14) is added as the mass of the “pendulum” is not a point mass and therefore gives resistance once rotated around its own centre.

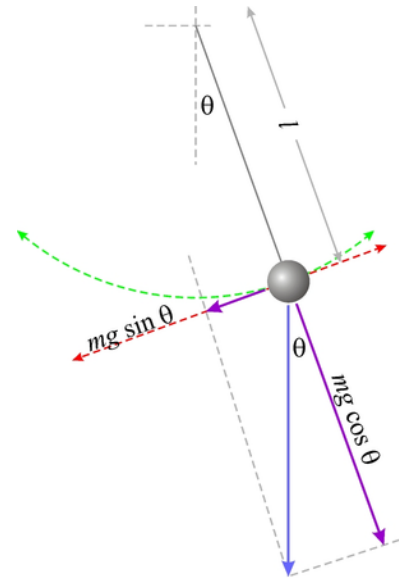


Figure 9: Pendulum

$$T = \frac{1}{2}ml^2\dot{\theta}^2 \quad (11)$$

$$V = -mgl \cos(\theta) \quad (12)$$

$$L = T - V, \quad \tau = \frac{d}{dt} \left(\frac{\partial L}{\partial \dot{\theta}} \right) - \frac{\partial L}{\partial \theta} \quad (13)$$

$$\tau = I\ddot{\theta} + ml^2\ddot{\theta} + mgl \sin(\theta) \quad (14)$$

The models have been tested in two situations; purely static postures and dynamic situations with different angles. The static situations all gave the same results, thus no difference between hand calculation and model output. The results for the dynamic situation can be seen in Table 2.

θ	$\ddot{\theta}$	Hand calculation	InvArm function	SimMechanics
0	π	0.0124	-0.0127	0.0082
$\pi/4$	π	0.2507	0.2255	0.2465
$\pi/2$	π	0.3493	0.3242	0.3452
π	π	0.0124	-0.0127	0.0082
0 or π	$3000\pi/180$	0.2065	-0.2122	0.1371
$\pi/4$	$3000\pi/180$	0.4448	0.0261	0.3753
$\pi/2$	$3000\pi/180$	0.5435	0.1247	0.4740

Table 2: Comparing hand calculation and InvArm function and SimMechanics model for different dynamic situations

From these results we can conclude that the models deviates from the hand calculated values. The reason for the sign difference in the InvArm function, for the situations where position is vertical, is not found. Besides this peculiar behaviour it can be noticed that an increased angular acceleration increases the difference between the hand calculation and the InvArm function. The SimMechanics model gives results closer to the hand calculated values for the angles $\pi/4$ and $\pi/2$. Because the SimMechanics model seems to produce better results, the inverse model in Simulink will be used to compute the torques.

6.4.1 Forward model

With the inverse dynamics model in Simulink, the input and output parameters can be changed to give a forward model. The joint actuators are now set to be driven by torques instead of angular position, velocity, and acceleration. For the joint sensors it is the other way around, where the measurement of torque is replaced by the measurement of the kinematic parameters.

7 Results

In this chapter the results from the upper limb model are discussed. The results are presented in roughly chronological order. First the behaviour of the forward model is explained based on model input and output. However due to a mistake, the initial conditions were not set. The importance of initial conditions is mentioned and new results are produced and discussed. Next it is investigated whether the sequence of the joints influence the behaviour of the model. Finally multi joint actuation is analysed.

7.1 Model behaviour

The inverse model has been used to create an input for the forward model. The inverse model has been checked, as described in the previous chapter, and can therefore be used in the analysis of the forward model. A sine function has been used as input for the angular position of one joint at the time. The sine function was differentiated twice to provide for the angular velocity and acceleration. The input sine function is presented in Figure 10.

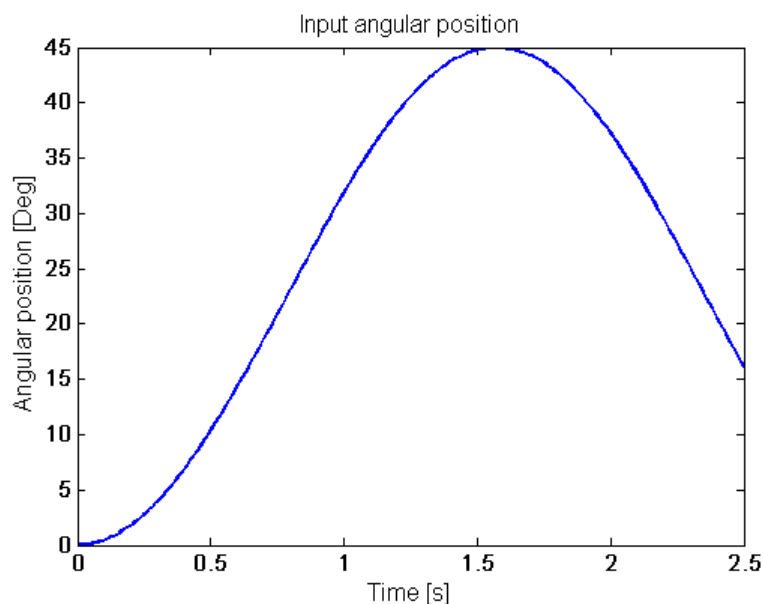


Figure 10: Angular input function

Each joint is actuated individually. This means that one joint was actuated with the sine function and its derivatives and the others were kept at zero angular position, velocity and acceleration. For shoulder flexion, the resulting torque profile and the response of the forward model to this torque can be observed in the next set of figures. Figure 11 shows the torque profile over time and Figure 12 the angular position output of the forward model.

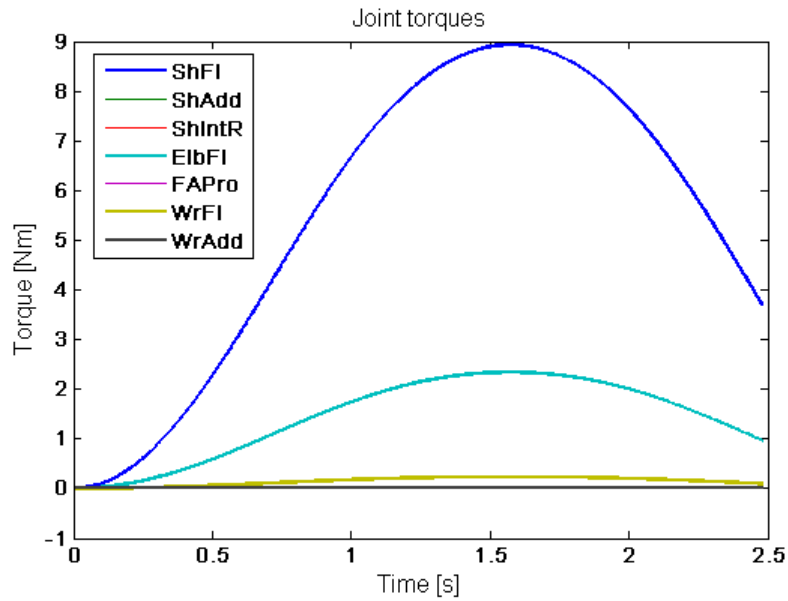


Figure 11: Forward model input torque profiles

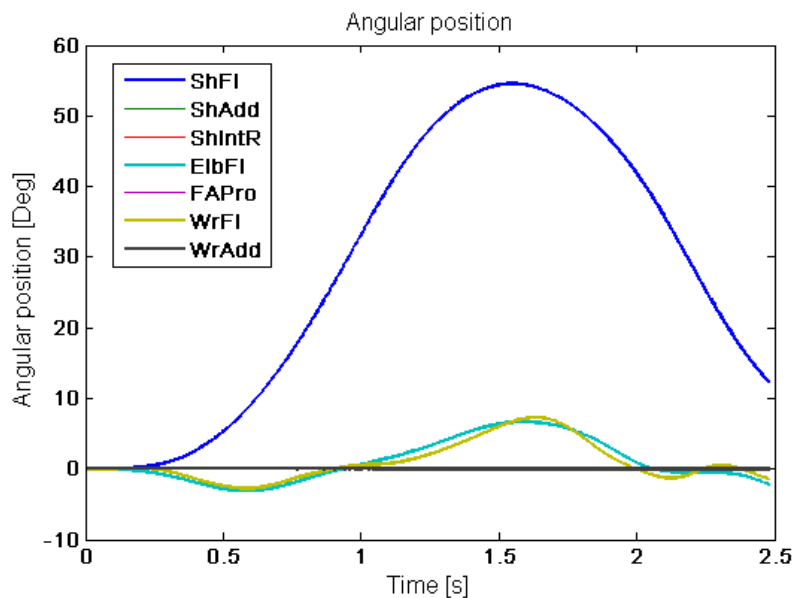


Figure 12: Forward model output angular positions

As can be seen in Figure 11, the torques profile for shoulder flexion has the same shape as the sine function. This can be explained by the fact that the moment arm of the moment around the shoulder is the distance from the shoulder joint centre to the combined centre of mass multiplied by the sine of the flexion angle.

The angular position resulting from the forward simulation however shows some differences with the original input function. First thing to notice is the delayed start of movement. This delay is crucial as it can be reasoned that the other differences are a direct consequence of this delay.

The extension of the elbow and wrist are the result of an overestimated flexion angle of the shoulder. As the input torque is processed with respect to its timing, the simulated position is lagging the position for which the torque is given. This results in a larger acceleration as the moment required is

lower than the moment fed to the system. The elbow and wrist torques are not computed with this increased shoulder flexion acceleration and therefore go into extension.

In the period where the shoulder is flexing, the acceleration grows a little more as the extended elbow and wrist reduce the moment arm of the combined centre of mass. This increased acceleration results in a larger maximum flexion angle occurring at the shoulder.

7.2 Initial conditions

For a forward dynamics calculation the initial conditions are important for the stability of the structure. The results in the previous paragraphs illustrate this, as the initial conditions were not used. To further illustrate the importance of the initial condition, a forward dynamics simulation has been performed with and without the initial conditions set. The input position profile of the inverse model was a part of a sine function. This input function can be seen in Figure 13. The initial conditions were obtained from this function and its derivative.

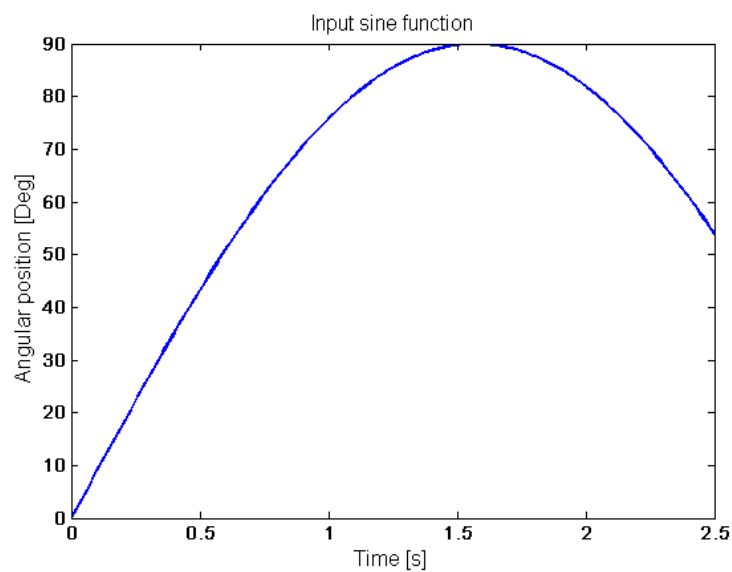


Figure 13: Input sine wave to test initial conditions

The input function is such that there is an initial velocity significantly larger than zero. The resulting output of the forward dynamics calculation without setting the initial conditions, thus initial conditions all zero, can be seen in Figure 14. Only the shoulder flexion joint was set to follow the input sine function.

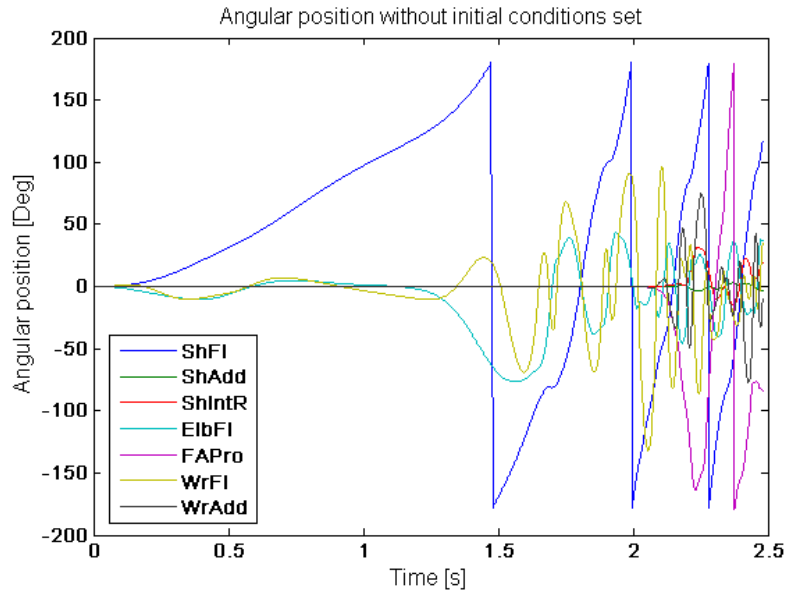


Figure 14: Forward model output without setting initial conditions

As can be seen from the figure, the angles of the different joints do not behave as desired. The shoulder flexion approaches the input function for the first second but after that increases, whereas the position angle of the input sine function reduces again. Setting the initial shoulder flexion velocity at the appropriate value gives much better result as can be seen in Figure 15.

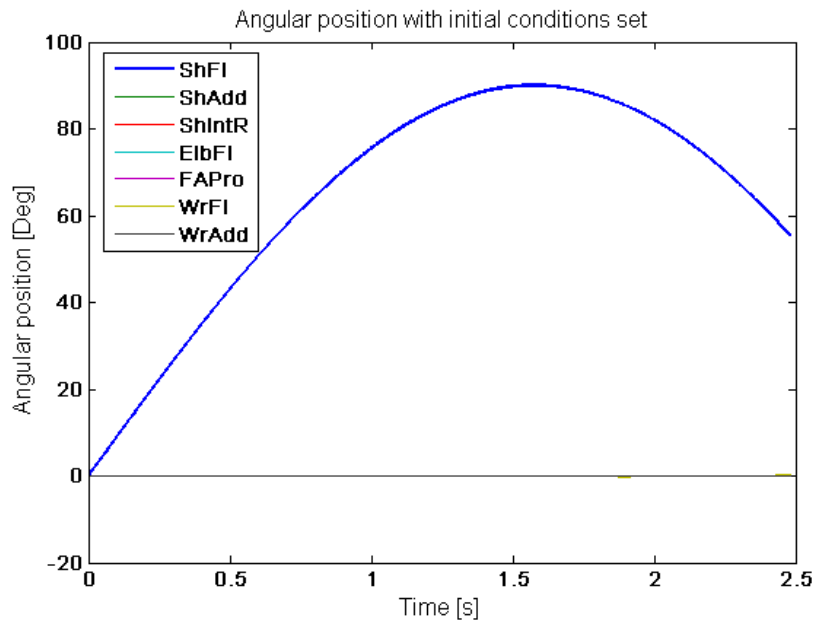


Figure 15: Forward model output after setting initial conditions

7.3 New results

The new results with the initial conditions set to the appropriate values are discussed in this section. A sine wave as shown in Figure 10 is used as the input for the inverse model shoulder flexion. Figure 16 and Figure 17 give the result of the inverse and the forward model respectively.

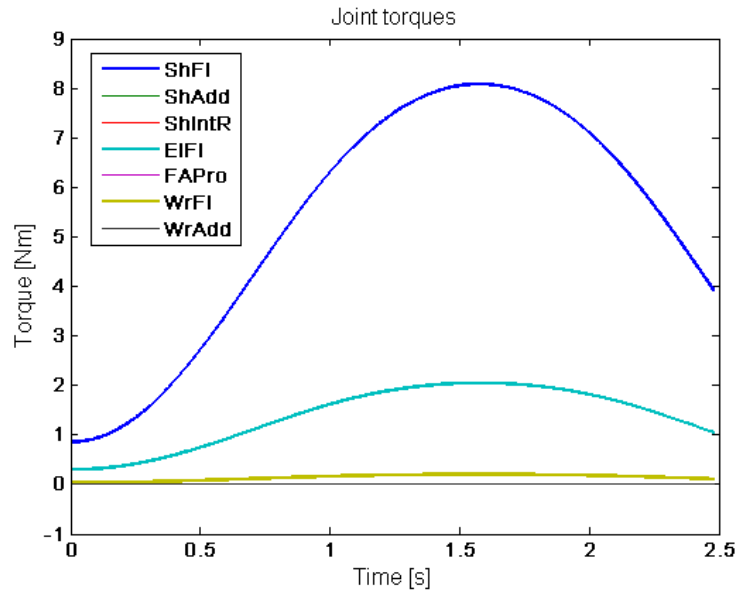


Figure 16: Forward model new input torque profiles

The joint torques are straightforward. The torque for shoulder flexion shows the same profile as the requested movement. Elbow flexion and wrist flexion torques are of equal shape but lower in amplitude as the mass distally from the joint is smaller. Figure 17 shows the resulting simulated movement. The simulated movement seems good. However there is a slight movement at the other flexion joints. This can be seen in Figure 18 where a crop of Figure 17 is presented. Despite the initial conditions there is still a small oscillation of the distal segments. To exclude the integrator as the cause for the behaviour, different integrators and time steps were analysed. These gave the same result and thus it can be said that the integrator or time step is not the cause for the unwanted movements. The results for the other joint movements can be found in Appendix IV.

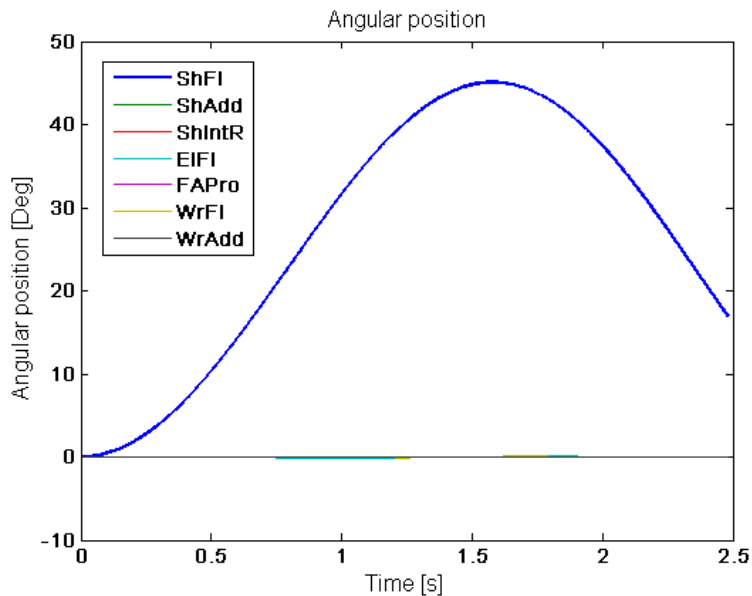


Figure 17: Forward model new result angular positions

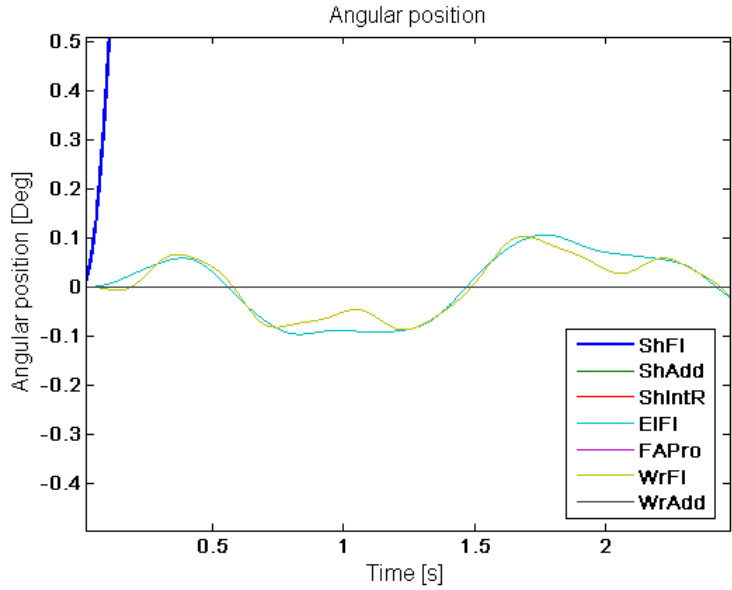


Figure 18: Forward model new result angular positions crop view

7.4 Sequence of revolute joints

To investigate whether the sequence of the revolute joints have influence on the stability and behaviour of the arm two additional sequences were processed and analysed. The original sequence serves as the reference. The second sequence has adduction and internal rotation in the shoulder, and flexion and pronation at the elbow, interchanged. The order of revolute joints of the third sequence is equal to the original apart from the interchanged pronation and flexion joint at the elbow. As in the analysis of the model behaviour, it is investigated for the actuation of each revolute joint individually. Figure 19 shows the angular position resulting from the forward simulation for the three different sequences for the case of the actuated shoulder adduction. Appendix V discusses the results for other joint actuations.

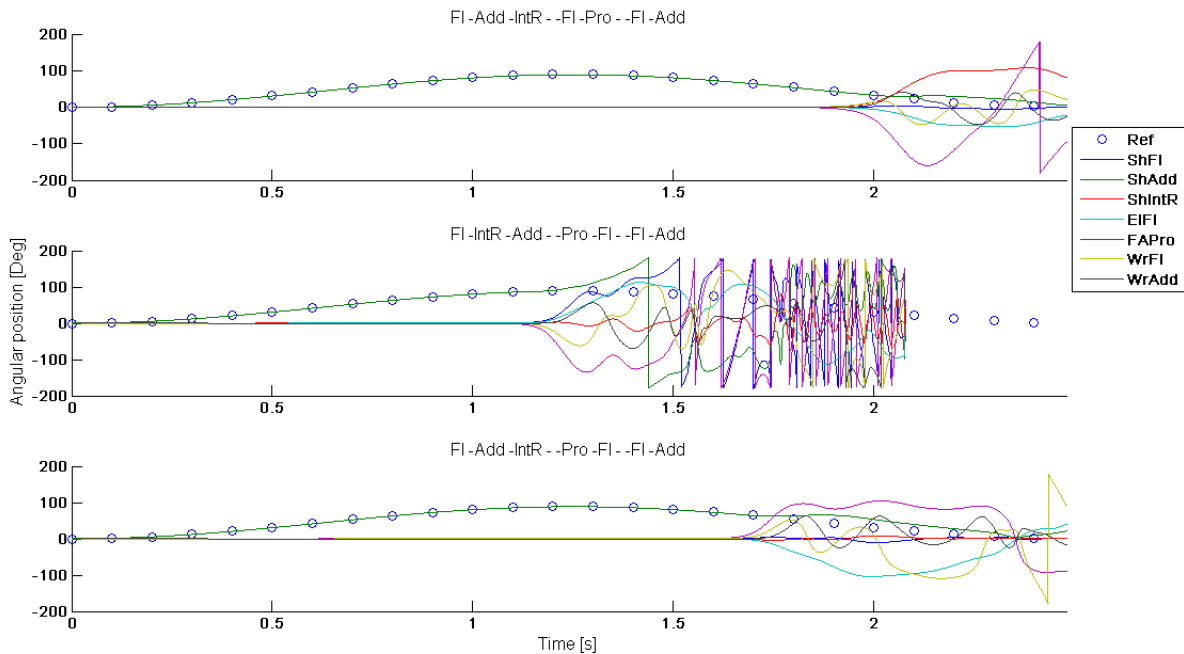


Figure 19: Forward model output for three joint sequences with; top: original reference sequence, middle: sequence 1, bottom: sequence 2

Looking at the graphs in Figure 19 it can be seen that all sequences give the same good behaviour for the first second. However the reference sequence shows the best result looking at the other joint movements. Near the end, or when the angle starts to deviate from the reference position, other joints start to act up more visibly. The area close to where the arm reaches the ninety degrees is also where the sequence seems to have an influence on the behaviour of the other joints. The second sequence encountered singularities in the simulation this stopped the simulation. A reason for this singularity could be a fast moving segment, causing the time step size to be insufficient. To solve this one could reduce the time step. This however increases the number of calculations and therefore computing time.

7.5 Multi actuation

Until now only one revolute joint was actuated for the analysis of the model. This section analyses multi actuation of the flexion joints. The result of actuated shoulder and elbow flexion is shown in Figure 20 followed by the result with co-activation of wrist flexion in Figure 21.

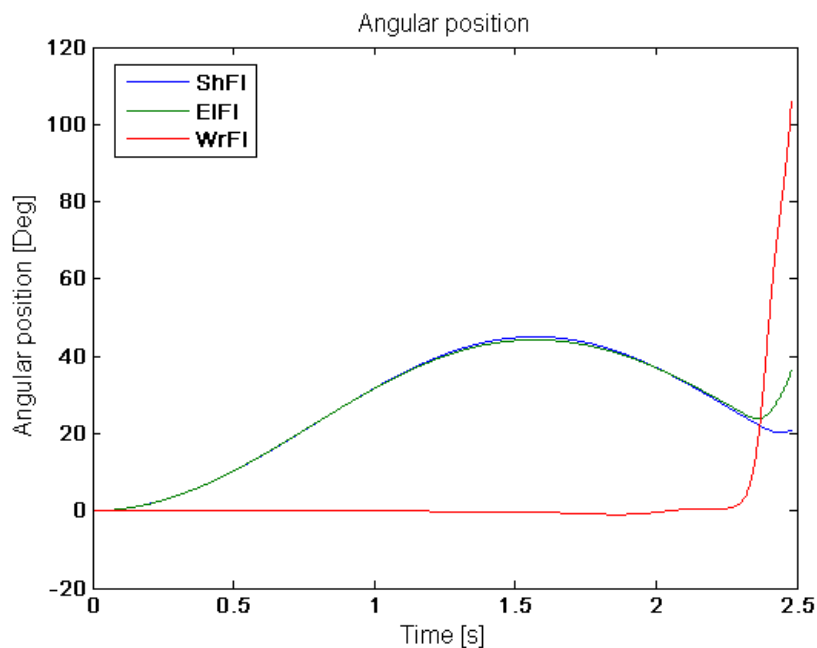


Figure 20: Forward model output with actuated shoulder and elbow flexion

The figure above shows the simulated movement of the arm where shoulder and elbow flexion are actuated. Looking at the graph it can be seen that the wrist starts moving with respect to the forearm after 1.2 seconds. Near the end of the 2.48 seconds runtime elbow flexion also starts to deviate from the desired path as wrist begins to rotate. The flexion at the wrist causes the total centre of mass of forearm and hand to shift to the elbow joint. Therefore the required torque to keep the distal segments at their position is lower than the torque exerted on the joint. The excess of torque makes the elbow flexion angle to increase and deviate from the reference position.

All three flexion joints actuated results in the movement seen in Figure 21. Up to one second the arm behaves according to the reference position. However when the joint angles cross the thirty degrees, the wrist starts to “fall” into extension. At the point where all three flexion joints are thirty degrees flexed, the hand segment is orientated horizontally. Increasing the flexion angles makes the hand to resemble an inverted pendulum and thus evoke instable behaviour.

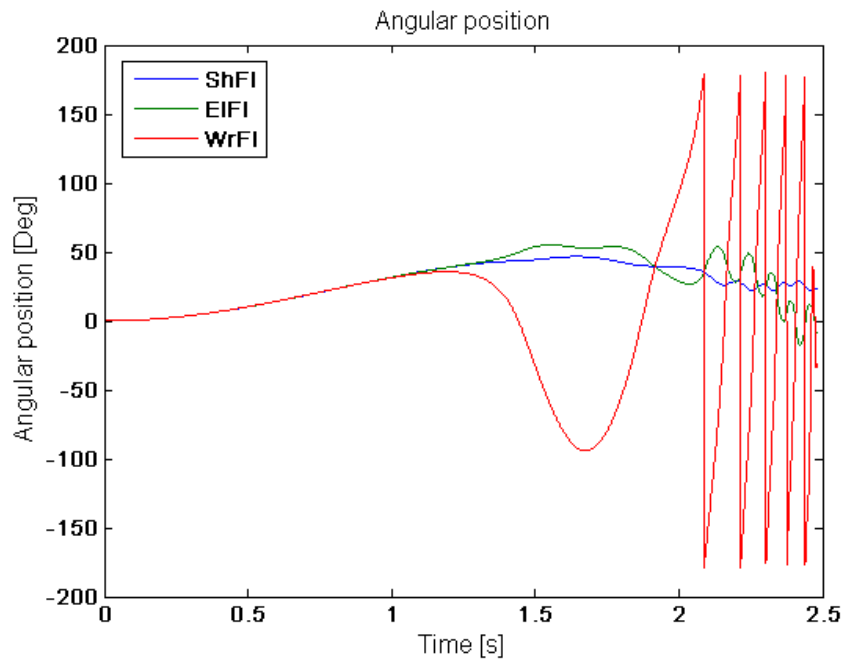


Figure 21: Forward model output for actuated shoulder, elbow, and wrist flexion

8 Discussion

This report mainly comprised the modelling of the upper limb. Modelling of the upper limb is important to better understand the relationship between impairment and human functioning. Partially this can be found by observing the patients however to understand the contribution of each of the mechanisms contributing to the impairment, modelling is essential. With an accurate model, for example, several neurological mechanisms can be tested separately. Eventually the model can be used to evaluate treatments before applying it to a patient, as the model can show the influence of a treatment to the ability to perform ADL. The model build is far from that final goal. The model discussed in this report was build to identify the problems arising from modelling in general and the issues concerning the forward dynamics simulation. This chapter discusses the modelling of the upper limb and the results from the inverse and forward models. Several notes are made on problems arising from the forward dynamics modelling and possible solutions are proposed. Recommendations are treated in the next chapter, future considerations.

8.1 Modelling of the upper limb

In the process of modelling the upper extremity, many assumptions were made to simplify the model. Most important assumption is the use of rigid bodies to model the segments of the upper limb. This makes the computational effort smaller but does not give the ability to accommodate for the changing muscle properties during movement. This change in muscle properties may change the inertia properties and the stiffness of the joints.

In terms of structure, the carrying angle at the elbow is not incorporated in the model as it changes with the flexion angle. Another simplification related to the structure is the definition of the joint centres. Joint centres are taken fixed but in reality they are changing over the range of movement(ROM) of the joint.

Other segment properties that kept the model basic was the exclusion of joint stiffness and boundaries on the joint ROM. Results should therefore be analysed critically, keeping in mind these simplifications. Adding joint stiffness would not simply result in an overall increase in required torques, as joint stiffness is related to the muscle properties and state of muscle activation. Joint ROM can be embedded by using an increasing damped resistance when getting closer to the limit.

All above mentioned simplifications affect the validity of the model. Although most of them are not embedded due to their complexity, restricted ROM was not implemented as it proved to be difficult in SimMechanics. The revolute joints accepted only one input and the ROM restriction block was seen as an input, making it the second input besides the torque actuation block.

In the first check with a hand calculation, unfortunately the InvArm function showed strange behaviour. It could not be retrieved where the sudden sign change originated from. The SimMechanics inverse dynamics model showed better results. Although it slightly deviated from the hand calculation it gave good results especially with angles of 45 and 90 degrees. Possible cause could be the different methods to define the coordinate frames, even though all coordinate frames are oriented equally.

8.2 Discussion on the results

In the results of the forward model, it could be seen that the initial conditions are of extreme importance. The SimMechanics model however only accounted for the initial position and velocity and not the initial acceleration. The small oscillation of the distal segments during actuation of the proximal segment might be the result of lack of this initial acceleration condition. Apart from this

reason, the oscillation might also occur due to an unforeseen fault in the model. Since the oscillations are a probable source of the system becoming unstable, certain factors influencing the stability of a system are investigated.

Integrator type and the time step used in the calculation have been excluded in section 7.3 as they showed no change in model behaviour. Since the segment parameters are all fixed and obtained from reliable sources, left to consider is the definition of the coordinate frames and the sequence of the revolute joints. From section 7.4 it can be seen that the sequence of the revolute joints does have an effect on the behaviour. However this is only for activation of shoulder adduction, creating an additional question of why only shoulder adduction movement is affected by joint sequence.

The coordinate frames and how they are defined form the base of the model. Several methods of defining the frames are possible in SimMechanics, Euler angles were chosen for ease of use. However the use of Euler angles introduces the gimbal lock phenomena when using three rotational degrees of freedom at one position, as used for the shoulder joint.

The creation of an inverted pendulum is most likely the largest contribution to instability. An inverted pendulum is by definition considered unstable. When the joint angles are such that one of the segments resembles an inverted pendulum, the model becomes unstable as could be seen in the multi actuated case where all three flexion revolute joints were activated. If the hand moves past the horizontal position it becomes an inverted pendulum and the time this occurs is also the time the hand starts to deviate from the reference position.

9 Future considerations

In the previous chapters the creation of a model of the upper extremity is discussed. However the model is far from perfect and there are many issues to be considered when proceeding with the modelling of the upper limb. This chapter comprises recommendations for further research on this subject.

With respect to the literature review and the method used to model the arm, the emphasis of the current literature review was on the analysis of upper limb kinematics and kinetics. This resulted in some valuable sources regarding segment parameters and range of the many kinematic and kinetic parameters during ADL. Due to the time constraint insufficient literature search has been done on the methods to model the upper limb. Although the current model gave an idea of the issues arising from modelling of the arm, more sophisticated models are developed which form a better base for future extension of the model with several packages like a muscle model and a neurological control system. A literature study on upper limb modelling is therefore recommended.

To prevent a very complex initial model it is advised to start with the basics and add more complexities to the model when the former model shows good behaviour. For now the rigid body approach is an accurate way to model the arm. When muscle models and neurological control systems are successfully implemented it might be worth trying to make the model with flexible bodies. The muscle model can be used for the generation of the parameters to define change in stiffness within the segments and in the joints.

For the development of a forward dynamics model emphasis is on finding a solution to the inevitable occurrence of instability. To increase the stability, integration algorithm and time step size should be selected carefully and feedback loops should be implemented. It is also recommended not to use Euler angles to define the coordinate frames.

The implementation of a neurological controller introduces several feedback loops. Even though there are many feedback loops the key ones to be considered will be the reflex and force feedback loops. Reflex loops giving positive feedback but opposing the movement and force feedback being negative feedback. These feedback loops will suppress undesired behaviour of the model and thus produce more stability. A neurological controller also gives the ability to model different neurological disorders, attributing to a better understanding of the disorder.

As can be read from the discussion, the Simulink package SimMechanics allows for a quick building of a model. However there are some restrictions to the package not preferable when modelling the upper limb. It should therefore be considered to use a different package, e.g. the robotics toolbox developed by Corke [20], or a complete different approach; not using Simulink.

It might also be fruitful to look at the computational algorithms used for lower limb modelling because it is similar to the upper limb, apart from the difference in degrees of freedom and range of movement. When all advice is taken in consideration, great progress can be made in modelling the upper limb, bringing the model closer to the end goal of using it to predict treatment result.

10 Reference list

1. Wikipedia. *Denavit-Hartenberg Parameters*. 2010 [cited 2010 November]; Available from: http://en.wikipedia.org/wiki/Denavit-Hartenberg_Parameters.
2. Davies, D.V. and F. Davies, *Gray's Anatomy*. 33 ed. 1962: Green & Co Ltd.
3. Marieb, E.N. and K. Hoehn, *Human anatomy and physiology*. 7th ed. 2007, San Francisco: Pearson Benjamin Cummings.
4. Wood, D.E., et al., *Biomechanical approaches applied to the lower and upper limb for the measurement of spasticity: A systematic review of the literature*. *Disability and Rehabilitation*, 2005. **27**: p. 19-32.
5. WEMOVE. *Spasticity*. 2009 [cited 2010 September]; Available from: <http://www.mdvu.org/library/disease/spasticity/>.
6. NINDS. *Stroke: Hope Through Research*. 2010 [cited 2010 September]; Available from: <http://www.ninds.nih.gov/disorders/stroke/stroke.htm>.
7. NINDS. *Cerebral Palsy: Hope Through Research*. 2010 [cited 2010 September]; Available from: http://www.ninds.nih.gov/disorders/cerebral_palsy/detail_cerebral_palsy.htm.
8. NINDS. *Spinal Cord Injury: Hope Through Research*. 2010 [cited 2010 September]; Available from: <http://www.ninds.nih.gov/disorders/sci/sci.htm>.
9. Malhotra, S., et al., *Spasticity, an impairment that is poorly defined and poorly measured*. *Clinical Rehabilitation*, 2009. **23**: p. 651-658.
10. Pandyan, A.D., *Spasticity*. 2010, Keele University: Keele.
11. Jacquier-Bret, J., N. Rezzoug, and P. Gorce, *Reach-to-grasp: a comparative study between C6-C7 quadriplegic and healthy subjects*. *Computer Methods in Biomechanics & Biomedical Engineering*, 2008. **11**(Journal Article): p. 119-120.
12. Gréa, H., M. Desmurget, and C. Prablanc, *Postural invariance in three-dimensional reaching and grasping movements*. *Experimental Brain Research*. *Experimentelle Hirnforschung*. *ExpAcrimtation CAcrAcbrale*, 2000. **134**(2): p. 155-162.
13. Marotta, J.J., W.P. Medendorp, and J.D. Crawford, *Kinematic Rules for Upper and Lower Arm Contributions to Grap Orientation*. *Journal of neurophysiology*, 2003. **90**(6): p. 3816-3827.
14. Murray, I.A. and G.R. Johnson, *A study of the external forces and moments at the shoulder and elbow while performing every day tasks*. *Clinical Biomechanics*, 2004. **19**: p. 586-594.
15. Kontaxis, A., et al., *A framework for the definition of standardized protocols for measuring upper-extremity kinematics*. *Clinical Biomechanics*, 2009. **24**: p. 246-253.
16. Buckley, M.A., et al., *Dynamics of the upper limb during performance of the tasks of everyday living--a review of the current knowledge base*. *Journal of Engineering in Medicine*, 1996. **210**: p. 241-247.
17. Morrey, B.F., L.J. Askew, and E.Y. Chao, *A biomechanical study of normal functional elbow motion*. *The Journal of Bone & Joint Surgery*, 1981. **63**: p. 872-877.
18. Barker, T.M., I.G. Kelly, and J.P. Paul, *Three-dimensional joint co-ordination strategies of the upper limb during functional activities*. *Journal of Engineering in Medicine*, 1996. **210**: p. 17-26.
19. Murray, I.A., *Determining Upper Limb Kinematics and Dynamics During Every Day Tasks*, in *Mechanical, Materials and Manufacturing Engineering*. 1999, University of Newcastle upon Tyne: Newcastle upon Tyne. p. 470.
20. Corke, P.I., *Machine Vision Toolbox*. *IEEE Robotics and Automation Magazine*, 2005. **12**(4): p. 16-25.
21. Vicon Motion Systems, *Plug-in-Gait Marker Placement*. 2010.
22. Naaij, A., *Working Space Representations for the Human Upper Limb in motion*, in *7th WSEAS Int. Conf. on APPLIED COMPUTER & APPLIED COMPUTATIONAL SCIENCE (ACACOS '08)*. 2008: Hangzhou, China. p. 394-399.

23. Swartz, N.M., *Arm Dynamics Simulation*. Journal of Robotic Systems, 1984. **1**(1): p. 83-100.
24. Vicon Motion Systems, *PIGModelling*. 2010.

I. Protocol

Introduction

In the pursuit of getting a better understanding of upper limb movements in humans, a model has been developed. With this model the torques in the joints can be computed given the joint angles, angular velocity and acceleration. With the movement data of a movement used in daily activities, the model can be verified with existing literature on this matter. This protocol is based on a framework for the definition of standardized protocols for measuring upper-extremity kinematics as proposed by Kontaxis et al. [15].

Joint / segment of interest

For the model input, joint kinematics is of interest. The numerical model consists of the three joints in the upper limb giving seven degrees of freedom. The glenohumeral, elbow, and wrist joints are the joints to be analysed. The glenohumeral joint is described with three degrees of freedom. Flexion/extension, abduction/adduction, and internal/external rotation of the upper arm. The movement of the scapula is not embedded and this movement should therefore be constrained during the measurement. This can be achieved by using a belt to keep the trunk in place. In the elbow joint the flexion/extension and the pronation/supination of the forearm are the two rotational DOFs. The wrist also has two degrees of freedom, flexion/extension and hand deviation.

Mechanical model of joints/ DOFs of segments

The focus of the study is joint kinematics. Therefore a mechanical equivalent of the joints is formulated. Figure 22 shows the linkages with the joints of interest and the DOFs of the joints. The three segments from proximal to distal end are upper arm, forearm and hand respectively. The joints: shoulder, elbow and wrist. The degrees of freedom are already discussed in the section above and therefore will not be repeated here.

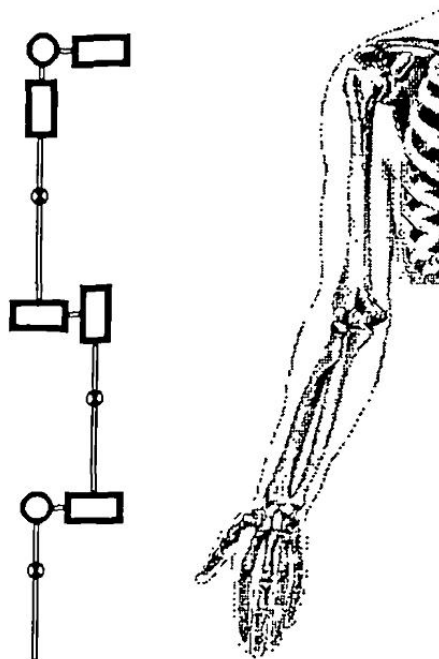


Figure 22: Technical representation of the arm

Joint / segment coordinate systems and angles

The joint and segment systems are inherited from the Vicon model.

Measurements on subject prior to data collection

- Subject weight
- Subject height
- Arm length
- Shoulder offset from sternum to shoulder joint centre/acromion
- Shoulder offset from acromion to joint centre. (Approx. from Murray(1999))
- Elbow and wrist joint width
- Hand thickness

Marker set-up / placement

For the marker set-up, the marker placements described by Vicon will be used. This gives the ability to use the Vicon software to process the collected data into a useful format. An overview and description of the marker placement of the upper body is given in the paragraphs below.

According to the Plug-in-Gait Marker Placements document [21], the markers for an upper body analysis should be placed on specific positions. For the upper body model to work the minimum requirement is the use of the markers on the thorax. Table 3 and Table 4 give the markers used on the head and the torso of the subject.

Head markers

LFHD	Left front head	Located approximately over the left temple
RFHD	Right front head	Located approximately over the right temple
LBHD	Left back head	Placed on the back of the head, roughly in a horizontal plane of the front head markers
RBHD	Right back head	Placed on the back of the head, roughly in a horizontal plane of the front head markers

Table 3: Position head markers

A headband can be used to attach the markers.

Torso Markers

C7	7 th Cervical Vertebrae	Spinous process of the 7th cervical vertebrae
T10	10 th Thoracic Vertebrae	Spinous Process of the 10th thoracic vertebrae
CLAV	Clavicle	Jugular Notch where the clavicles meet the sternum
STRN	Sternum	Xiphoid process of the Sternum
RBAK	Right Back	Placed in the middle of the right scapula. This marker has no symmetrical marker on the left side. This asymmetry helps the auto-labelling routine determine right from left on the subject.

Table 4: Position of torso markers

C7, T10, CLAV, STRN define a plane hence their lateral positioning is most important.

The markers remaining are those on the arm, which are given in Table 5.

Arm Markers

LSHO	Left shoulder marker	Placed on the Acromio-clavicular joint
LUPA	Left upper arm marker	Placed on the upper arm between the elbow and shoulder markers. Should be placed asymmetrically with RUPA
LELB	Left elbow	Placed on lateral epicondyle approximating elbow joint axis
LFRA	Left forearm marker	Placed on the lower arm between the wrist and elbow markers. Should be placed asymmetrically with RFRA
LWRA	Left wrist marker A	Left wrist bar thumb side
LWRB	Left wrist marker B	Left wrist bar pinkie side
LFIN	Left fingers	Actually placed on the dorsum of the hand just below the head of the second metacarpal

Table 5: Arm markers

The wrist markers are placed at the ends of a bar attached symmetrically with a wristband on the posterior of the wrist, as close to the wrist joint centre as possible.

Where left side markers only are listed, the positioning is identical for the right side.

The interest lies in single arm movements this means that only one arm is used in the movement analysis. However the markers will be placed on both arms to make sure the Vicon upper body model will process the data. The non-dominant hand will remain on the table.

A visual representation of the marker placement can be found in Figure 27.

Initial static trial

Since the T10 marker will be in the way when sitting on a chair it should be created virtually. To replace the T10 marker, three markers are required to produce a virtual marker in a static trial. C7, STRN, and a marker on the base of the sternum are the three markers used for this. An initial standing trial is used to calibrate the T10 marker position with respect to the three reference markers. The T10 marker can then be removed for the dynamic tests.

Set of activities to be measured

To compare the output of the numerical model with the literature, an identical task as those performed in literature should be used. The movement of bringing the hand to the mouth is the most common used in daily activities. Either while eating, when a person brings the food with or without tool to the mouth, or while drinking, when it brings a cup to the mouth.

The initial position of the arm is with the hand flat on a table. Elbow approx. 90 degrees in line with the shoulder. Reach to grasp “food” 20cm straight ahead of the initial hand position. Then the food is taken to the mouth without moving the head. To make the movement as real as possible, it is advised to use real food. Short bread cakes for example.

If there is time left, three additional movements will be recorded as they are also important in daily live activities.

- The second movement is the hand to top of the head. The initial position will be equal to the eating movement. The end of the movement will be when the hand is flat on the top of the head.
- The third movement will be a reach movement in which the subject will point forwards to a pre-defined position. With an initial position of the hands flat on the table, in line with the shoulder.
- The fourth movement to analyse is a reach to the back movement. Again the same initial position as the previous movements. However for ease it might be best to use a chair without a back. Keeping the trunk steady will be instructed.

Estimation of time

The individual movements themselves will be about 2 seconds. Taking in consideration the rest time and the time to stop and start a new measurement it probably takes half a minute for one movement. If we take the same approach as Murray and Johnson[14], ten repetitions for each movement should be performed in order to get a data set describing a movement that is as natural as possible. To get enough data 15 repetitions will be done of each movement, resulting in a total of 60 movements. This means the movement recording on itself would take about thirty minutes. Including the marker positioning and the set change for the reach to back movement, an hour should be sufficient time for one subject to perform the movements and for us to collect the data.

Relation between marker and underlying skeletal structure

For the relation of the markers to the underlying structure, again the approach of Vicon [24] has been taken as a guideline. The paragraphs below describe the approach to get the underlying structure as it is processed in Vicon software.

Fixed Values

A Shoulder offset value is calculated from the Subject measurement value entered, plus half the marker diameter. Elbow, Wrist and Hand offset values are also calculated from the sum of the respective thickness with the marker diameter divided by two.

A progression frame is independently calculated in just the same way as for the lower body. C7 is tested first to determine if the subject moved a distance greater than the threshold. If not, the other thorax markers T10 CLAV and STRN are used to determine the general direction the thorax was facing in from a mean of 10% of the frames in the middle of the trial.

The "Chord" function

This function is used extensively in models for defining joint centres. Three points are used to define a plane. One of these points is assumed to be a previously calculated joint centre, and a second is assumed to be a real marker, at some known, perpendicular distance (the Joint Centre Offset) from the required joint centre. Also see Figure 23.

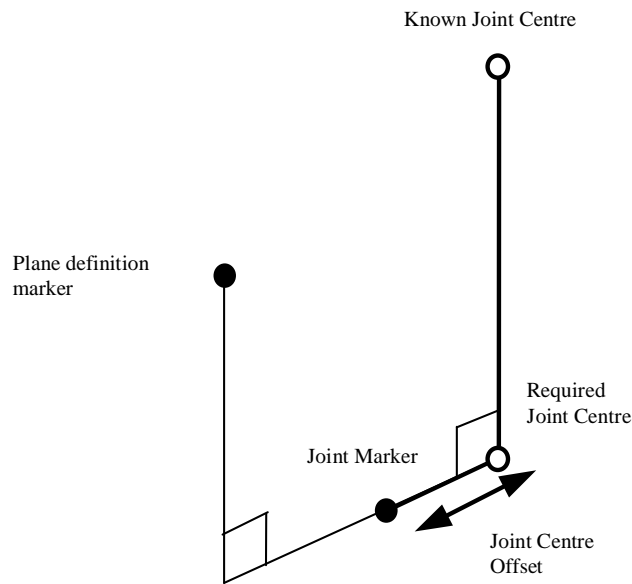


Figure 23: Chord function graphical example

It's called a chord because by definition, the three points (two joint centres and the joint marker) lie on the periphery of a circle.

There is also a modified version of the function, which calculates the required joint centre position when the plane definition marker is rotated out of this plane by a known angle round the proposed joint centre axis.

Thorax

The orientation of the thorax is defined before the origin. The Z axis, pointing upwards, is the predominant axis. This is defined as the direction from the midpoint of the STRN and T10 to the midpoint of CLAV and C7. A secondary direction pointing forwards is the midpoint of C7 and T10 to the midpoint of CLAV and STRN. The resulting X axis points forwards, and the Y axis points leftwards.

The thorax origin is then calculated from the CLAV marker, with an offset of half a marker diameter backwards along the X axis.

Shoulder Joint Centre

The clavicles are considered to lie between the thorax origin, and the shoulder joint centres. The shoulder joint centres are defined as the origins for each clavicle. Note that the posterior part of the shoulder complex is considered too flexible to be modelled with the used marker set.

Initially a direction is defined, which is perpendicular to the line from the thorax origin to the SHO marker, and the thorax X axis. This is used to define a virtual shoulder 'wand' marker.

The chord function is then used to define the shoulder joint centre (SJC) from the Shoulder offset, thorax Origin, SHO marker and shoulder 'wand'. A graphical representation can be seen in Figure 24.

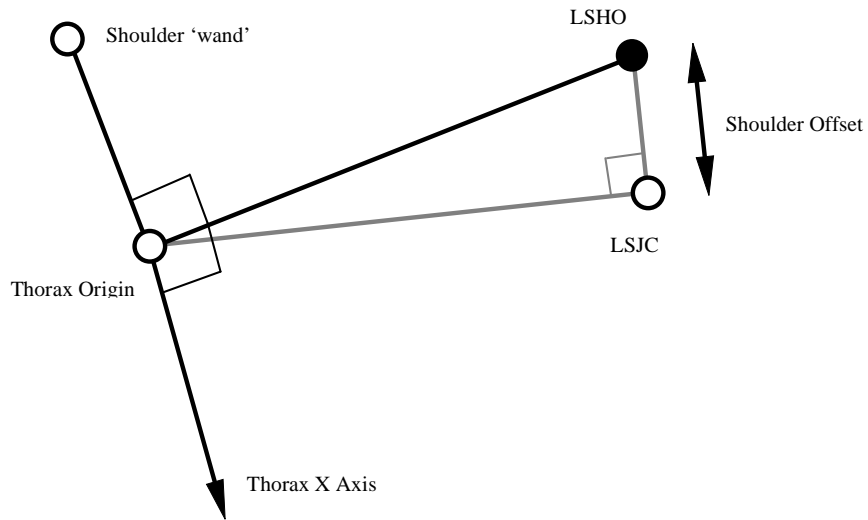


Figure 24: Shoulder joint centre

Elbow Joint Centre

A construction vector direction is defined, being perpendicular to the plane defined by the shoulder joint centre, the elbow marker (LELB) and the midpoint of the two wrist markers (LWRA, LWRB) as can be seen in Figure 25.

The elbow joint centre is defined using the chord function, in the plane defined by the shoulder joint centre, the elbow marker and the previously defined construction vector.

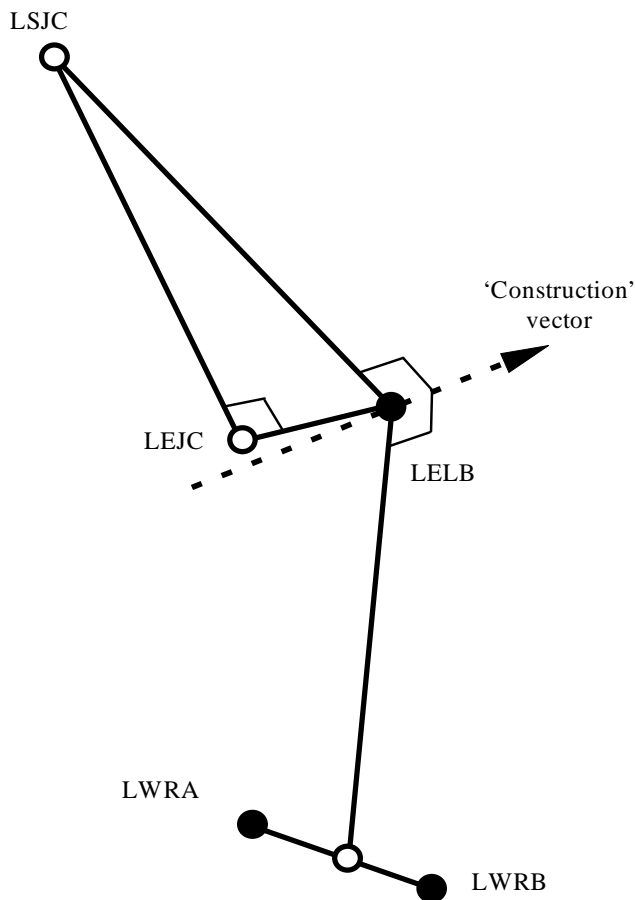


Figure 25: Elbow joint centre

Wrist Joint Centre

The wrist joint centre (WJC) is then calculated. In this case the chord function is not used. As depicted in Figure 26, the wrist joint centre is simply the offset from the midpoint of the wrist bar markers along a line perpendicular to the line along the wrist bar, and the line joining the wrist bar midpoint to the elbow joint centre.

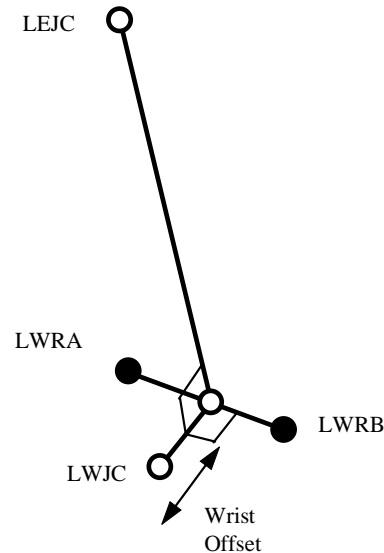


Figure 26: Wrist joint centre

Humerus

The Humerus is then defined with its origin at the EJC, a principal Z axis from EJC to SJC, and a secondary line approximating to the X axis between the EJC and the WJC.

Radius

The radius origin is set at the wrist joint centre. The principal axis is the Z axis, from the WJC to the EJC. The secondary line approximating to the Y axis is taken as the Y axis of the Humerus segment.

Hand

The hand is defined by first defining its origin. The chord function is used again for this, with the WJC, FIN marker and Hand Offset. The midpoint of the wrist bar markers is used to define the plane of calculation.

The principal Z axis is then taken as the line from the hand origin to the WJC, and a secondary line approximating the Y axis is defined by direction of the line joining the wrist bar markers.

Data processing

In vicon software the trials are reconstructed to produce marker trajectories. The trajectories are labelled to identify the trajectories to anatomical location. The data will be passed through a low pass filter to smooth the motion.

Also the static trial will be processed to calibrate the position of T10. Each dynamic trial is processed to put in the virtual T10. Finally the dynamic trial data will be processed using the dynamic plug in gait vicon software.

II. Matlab InvArm function

This appendix contains the program code of the InvArm function used to compute the joint torques required to move the arm through inverse dynamics.

```
function TAU = InvArm(THETA, DTHETA, DDTHETA)
%{
Function for inverse dynamics. It computes the torques necessary for the
given movement.

Model of the upper limb with use of Denavit-Hartenberg parameters.

Source for the equations:
    Swartz, Neil M., Arm Dynamics Simulation, Nov. 1982.
Parameters of the human body retrieved from:
    Determining Upper Limb Kinematics and Dynamics During Everyday Tasks
    Ingram A. Murray, B.Sc. (Hons.), M.Sc.
    Centre for Rehabilitation and Engineering Studies
    Department of Mechanical, Materials and Manufacturing Engineering
    University of Newcastle upon Tyne
    November 1999
%}
%% Input

theta = THETA;
dtheta = [0; DTHETA; 0];
ddtheta = [0; DDTHETA; 0];

%% Parameters

NL = 8;           %Number of links
%making space for the many vectors for speed purposes
w = zeros(3,NL);
dw = zeros(3,NL);
v = zeros(3,NL);
dv = zeros(3,NL);
dvm = zeros(3,NL);
s = zeros(3,NL);
p = zeros(3,NL);
f = zeros(3,NL+1);
n = zeros(3,NL+1);
F = zeros(3,NL);
N = zeros(3,NL);
tau = zeros(1,NL);

%Body parameters
BH = 1.80;       %Body height in m.
BW = 80;         %Body weight in kg.
lua = 0.174*BH;  %Length of upper arm
lfa = 0.156*BH; %length of fore arm
lh = 0.1079*BH; %length of hand
lc = 0.2;        %offset from earth coordinate frame to shoulder joint
mua = 0.0271*BW; %Mass of the upper arm
mfa = 0.0162*BW; %Mass of the forearm
mh = 0.0061*BW; %Mass of the hand
cmua = 0.5772*lua; %Centre of mass of the upper arm from proximal joint
cmfa = 0.4574*lfa; %Centre of mass of the forearm from proximal joint
cmh = 0.3624*lh;  %Centre of mass of the hand from proximal joint
% D-H Parameters to describe the current coordinate frame with respect to the
previous coordinate frame.
a = [0 0 0 0 0 -lh 0]'; %length of common normal
th = [0 theta(1)+pi/2 theta(2)+pi/2 theta(3)+pi/2 theta(4) theta(5)
theta(6)+pi/2 theta(7) 0]'; %theta, angle about Z_n-1, from X_n-1 to X_n
d = [-lc 0 0 -lua 0 -lfa 0 0 0]'; %offset along Z_n-1 to common normal
alfa = [0 pi/2 pi/2 pi/2 -pi/2 pi/2 pi/2 pi/2 0]'; %angle about common normal, from
Z_n-1 to Z_n
```

```

%because matlab doesn't work with index zero there is a base link described
%wrt the BASE. Also for the external force and moments there is an extra
%link needed at the most distal part which is basically the same as the
%most distal link itself therefore another set of zero's.
DH = [th d a alfa];

%Dynamic Parameter set
m = [0 0 mua 0 mfa 0 0 mh]';
cx = [0 0 0 0 0 0 0 cmh]';
cy = [0 0 0 0 0 0 0 0]';
cz = [0 0 -cmua 0 -cmfa 0 0 0]';
b = [0 0 0 0 0 0 0 0]';
K1 = [0.285 0.276 0.288]';
K2 = [0.269 0.265 0.235]';
K3 = [0.158 0.121 0.184]';
Ixx = [0 0 mua*(K2(1)*cmua)^2 0 mfa*(K1(2)*cmfa)^2 0 0 mh*(K3(3)*cmh)^2]';
Iyy = [0 0 mua*(K1(1)*cmua)^2 0 mfa*(K2(2)*cmfa)^2 0 0 mh*(K1(3)*cmh)^2]';
Izz = [0 0 mua*(K3(1)*cmua)^2 0 mfa*(K3(2)*cmfa)^2 0 0 mh*(K2(3)*cmh)^2]';

DP = [m cx cy cz Ixx Iyy Izz b];

J = DP(:,[5 6 7])';
g = 9.81;

% Initial parameters
Z0 = [0 0 1]'; %Direction of Z axis.

w(:,1) = [0 0 0]'; %Angular velocity base link
dw(:,1) = [0 0 0]'; %Angular acceleration base link
v(:,1) = [0 0 0]'; %Linear velocity base link
dv(:,1) = [0 -g 0]'; %Linear acceleration base link

f(:,NL+1) = [0 0 0]'; %External force on most distal segment
n(:,NL+1) = [0 0 0]'; %External torque on most distal segment

%% Link velocities and accelerations
%Angular (w) and Linear (v) velocities and accelerations of the links
p(:,1) = [a(1) d(1)*sin(alfa(1)) d(1)*cos(alfa(1))]';
for i=1:NL-1;
    p(:,i+1) = [a(i+1) d(i+1)*sin(alfa(i+1)) d(i+1)*cos(alfa(i+1))]';
    w(:,i+1) = RotM(DH,i+1)*(w(:,i) + Z0*dtheta(i+1));
    dw(:,i+1) = RotM(DH,i+1)*(dw(:,i) + Z0*ddtheta(i+1) +
    cross(w(:,i), (Z0*dtheta(i+1))));
    v(:,i+1) = cross(w(:,i+1),p(:,i+1)) + RotM(DH,i+1)*v(:,i);
    dv(:,i+1) = cross(dw(:,i+1),p(:,i+1)) +
    cross(w(:,i+1),cross(w(:,i+1),p(:,i+1))) + RotM(DH,i+1)*dv(:,i);
end

%disp(p);
%Linear acceleration of centres of mass
%Acceleration of the centre of mass of a link
for i=1:NL
    s(:,i) = [DP(i,2) DP(i,3) DP(i,4)]';
    dvm(:,i) = cross(dw(:,i),s(:,i)) + cross(w(:,i),cross(w(:,i),s(:,i))) +
    dv(:,i);
end

%% Forces and Moments
for i=NL:-1:1
%Net forces and moments
%Total Force at link mass and total Moment about link coordinate origin
F(:,i) = DP(i,1)*dvm(:,i);

```

```

    N(:,i) = J(:,i).*dw(:,i) + cross(w(:,i),(J(:,i).*w(:,i)));
end
%Local forces and moments
%Forces and moments of adjoining links
for i=NL:-1:1
    f(:,i) = RotM(DH,i+1)*f(:,i+1) + F(:,i);
    n(:,i) = RotM(DH,i+1)*n(:,i+1) + cross(p(:,i),(RotM(DH,i+1)*f(:,i+1))) +
        cross(s(:,i),F(:,i)) + N(:,i);

end

%% Joint torques
%Torques about the link coordinate origin
for i=NL:-1:1

    tau(i) = n(:,i)'*(RotM(DH,i)'*Z0) + b(i)*dtheta(i);

end
%% Output

TAU = tau([2:8])';

% Additional Function to create the rotational matrices
function [RM]=RotM(DH,i)

theta = DH(i,1);
d = DH(i,2);
a = DH(i,3);
alfa = DH(i,4);

Rt = [cos(theta) -sin(theta) 0 0;
      sin(theta) cos(theta) 0 0;
      0          0          1 0;
      0          0          0 1];

Td = [1 0 0 0;
      0 1 0 0;
      0 0 1 d;
      0 0 0 1];

Ta = [1 0 0 a;
      0 1 0 0;
      0 0 1 0;
      0 0 0 1];

Ra = [1 0          0          0;
      0 cos(alfa) -sin(alfa) 0;
      0 sin(alfa) cos(alfa) 0;
      0 0          0          1];

TM = Rt*Td*Ta*Ra;
RM = TM([1 2 3],[1 2 3]);

```


IV. Model behaviour

In chapter seven the model behaviour for shoulder flexion is explained. The other degrees of freedom will be discussed in this appendix. The sine input function used for the shoulder flexion is also applied on the other revolute joints. For easy comparison the input sine function is displayed in Figure 28. For each degree of freedom two figures are presented, the first showing the joint torques computed by the inverse model, and the second figure gives the angular positions of the joints resulting from the forward dynamics simulation.

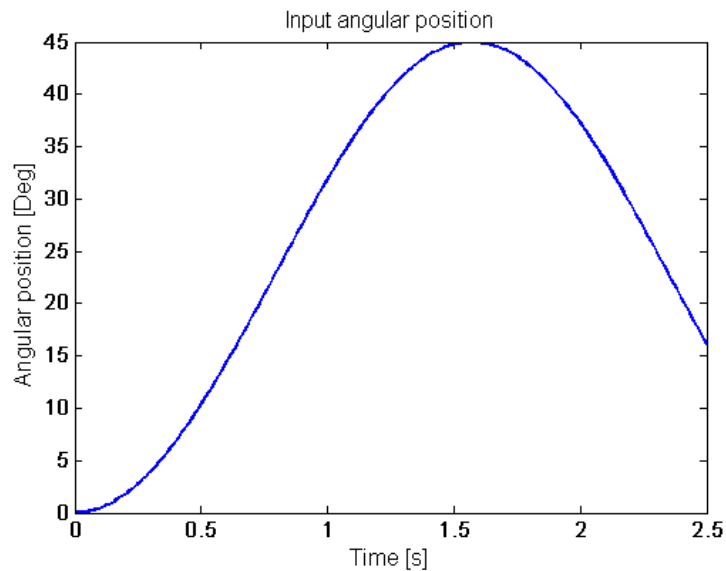


Figure 28: Input sine function

Shoulder adduction

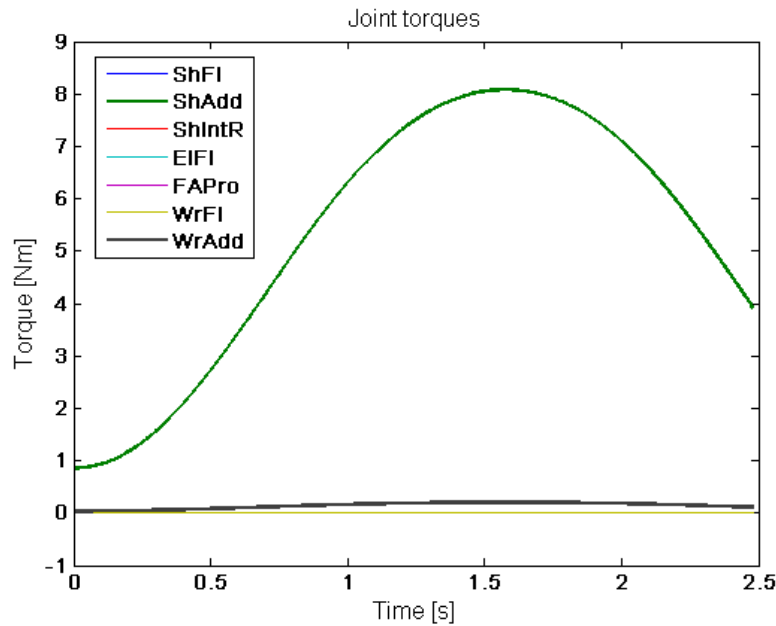


Figure 29: Joint torques for shoulder adduction

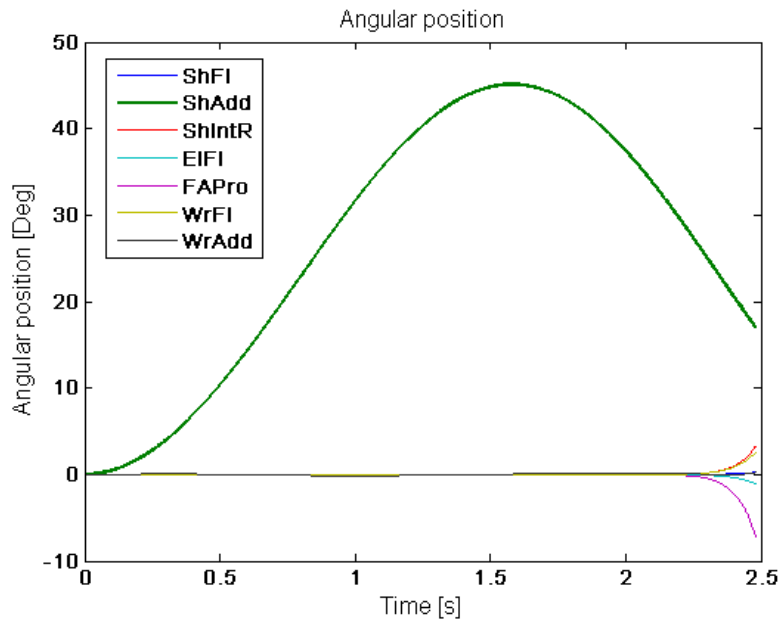


Figure 30: Angular position for shoulder adduction

Like the results with the shoulder flexion discussed in section 7.3, joint torques of shoulder adduction, which can be seen in Figure 29, follows the same shape as the input sine. This can again be explained by the fact that the moment arm of the moment around the shoulder is the distance from the shoulder joint centre to the combined centre of mass times the sine of the flexion angle.

Looking at the angular positions resulting from the forward simulation in Figure 30, it can be noticed that at the end of the movement all other joint movements kick in resulting in a chaotic movement. This sudden activation of the other joints might be initiated by the small oscillation of the hand in adduction. The torques for the not adduction movements are zero, therefore a slight deviation from zero will result in a free movement that is no longer controlled.

Shoulder internal rotation

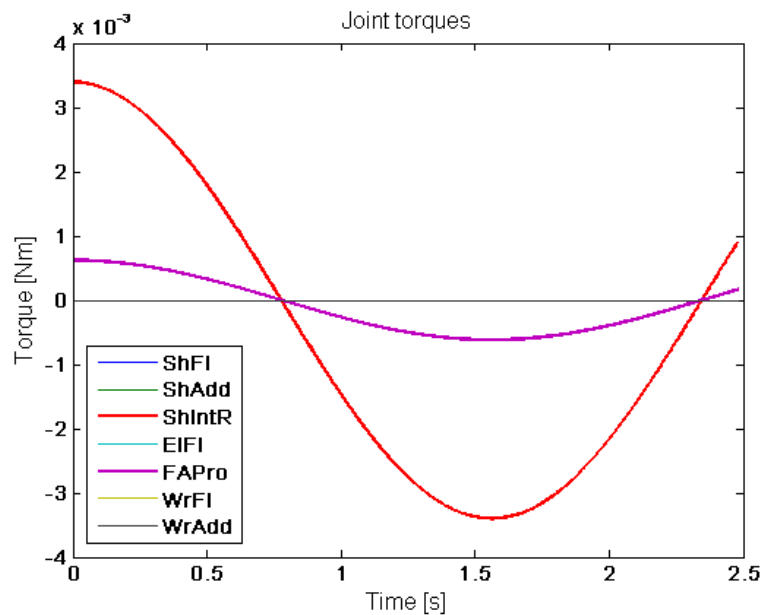


Figure 31: Joint torques for shoulder internal rotation

It can be seen in Figure 31 that the torques for shoulder rotation are very different from the torques for adduction and flexion movements. This can be explained by the not changing moment of inertia. The profile produces an acceleration of the limb, followed by a deceleration to reduce the rotation and to reverse the direction of rotation. No other joints are moving and thus the movement is very stable, as can be observed in Figure 32.

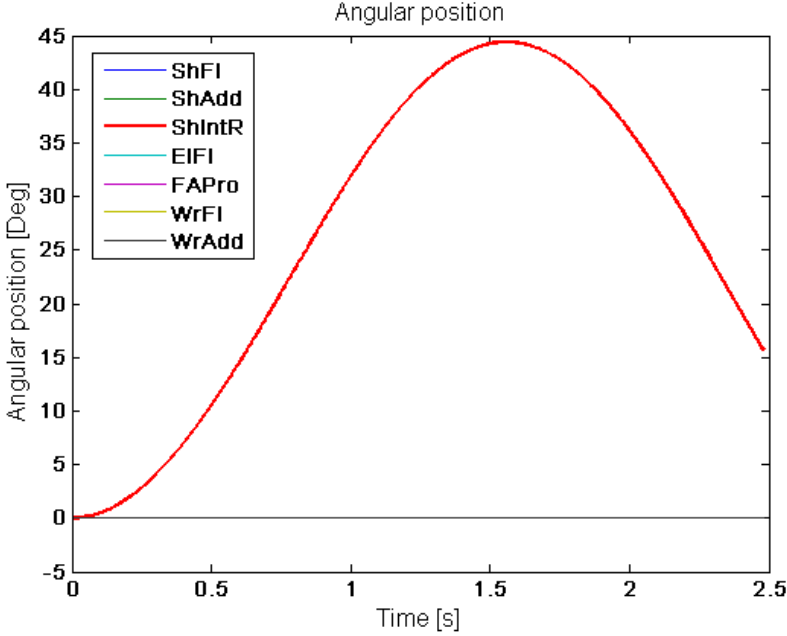


Figure 32: Angular position for shoulder internal rotation

Elbow flexion

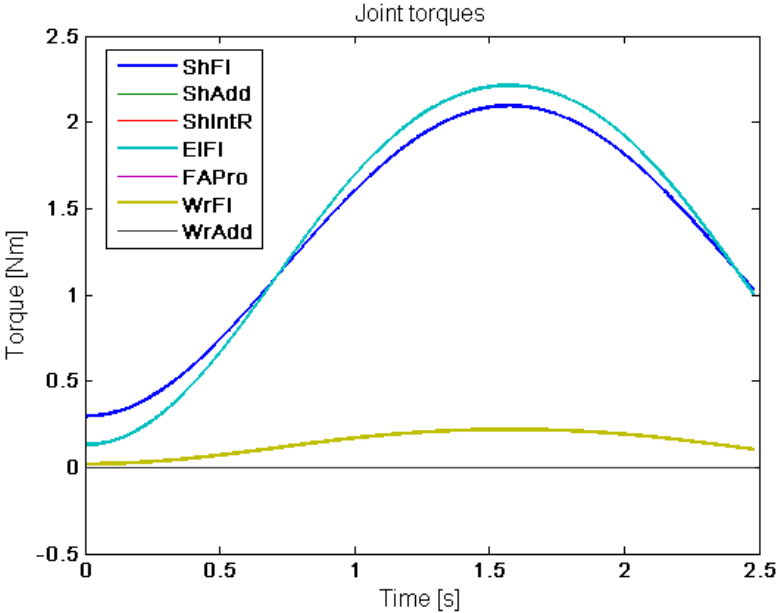


Figure 33: Joint torques for elbow flexion

Figure 33 shows the joint torques required to perform an elbow flexion movement. Elbow and shoulder flexion torques are both of the same magnitude because the moment around the elbow, to flex the elbow joint, is transferred to the shoulder joint where the reaction torque should be opposed to keep the arm in a fixed position. The mass of the upper arm causes the difference between the two

joint torque profiles, as shoulder torque does has to account for the upper arm mass and elbow torque not.

The resulting movement simulated is shown in Figure 34. The elbow joint does what it should however other joints are moving as well. When looking carefully it can be seen that the wrist is flexing. The shoulder is oscillating as well but both wrist and shoulder flexion, do not exceed oscillation amplitude of 0.1 degrees.

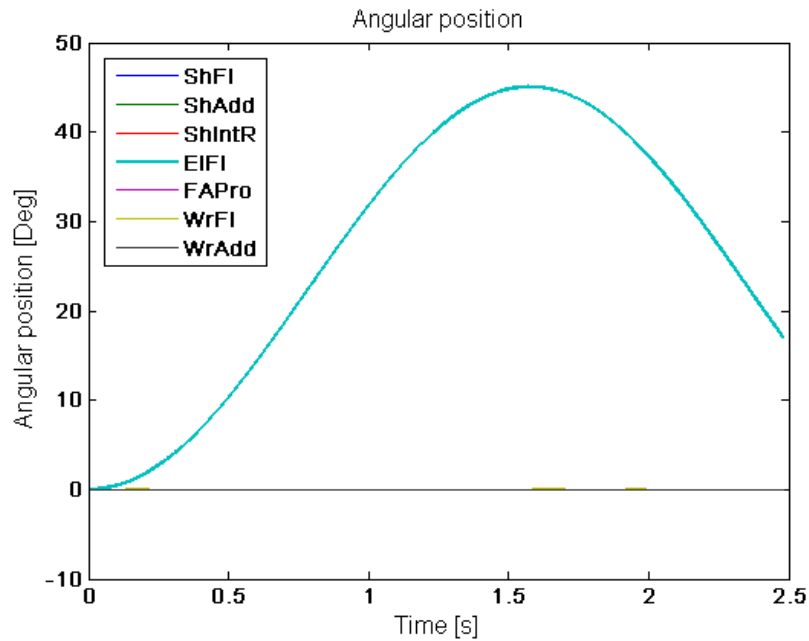


Figure 34: Angular position for elbow flexion

Forearm pronation

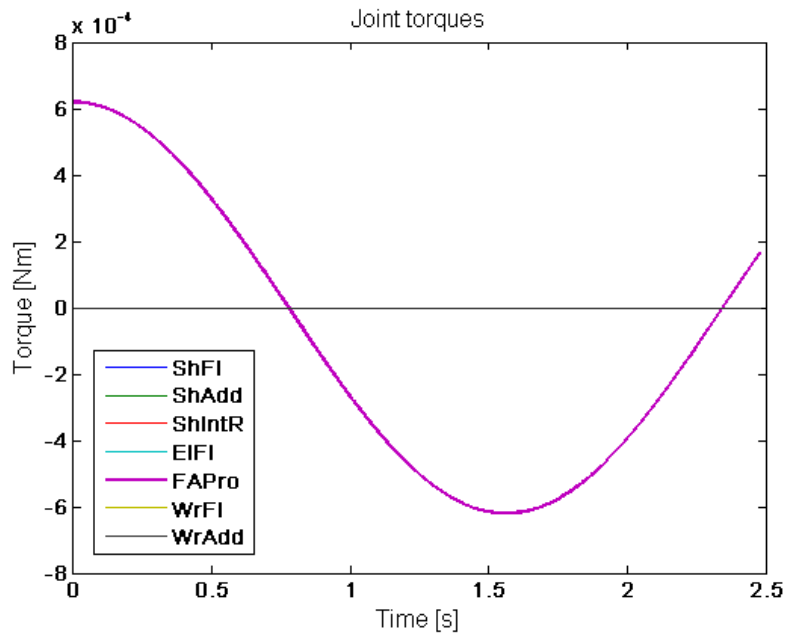


Figure 35: Joint torques for forearm pronation

Here again a familiar torque profile, to be seen in Figure 35, for the rotation of the forearm. The forward model results in a good replication of the input function, seen in Figure 36. No other revolute joints are active.

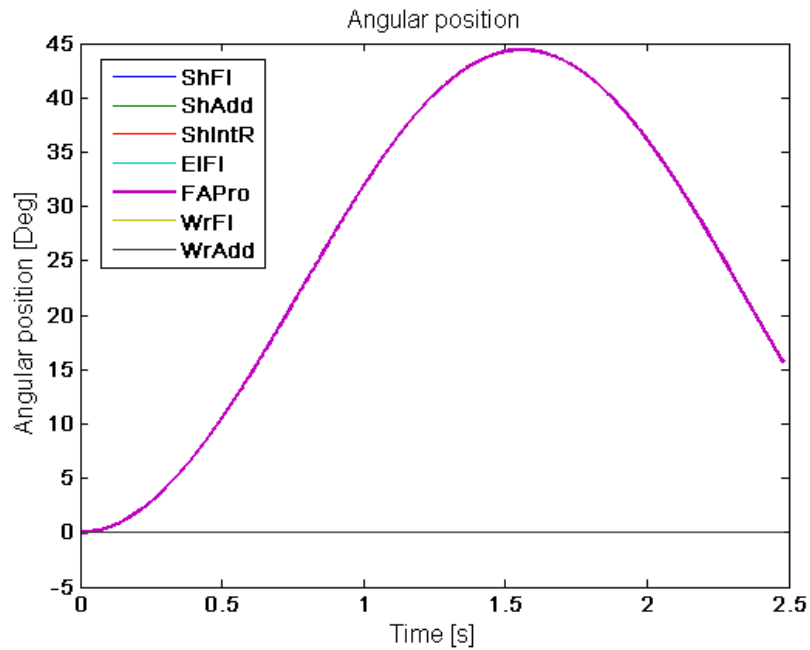


Figure 36: Angular position for forearm pronation

Wrist flexion

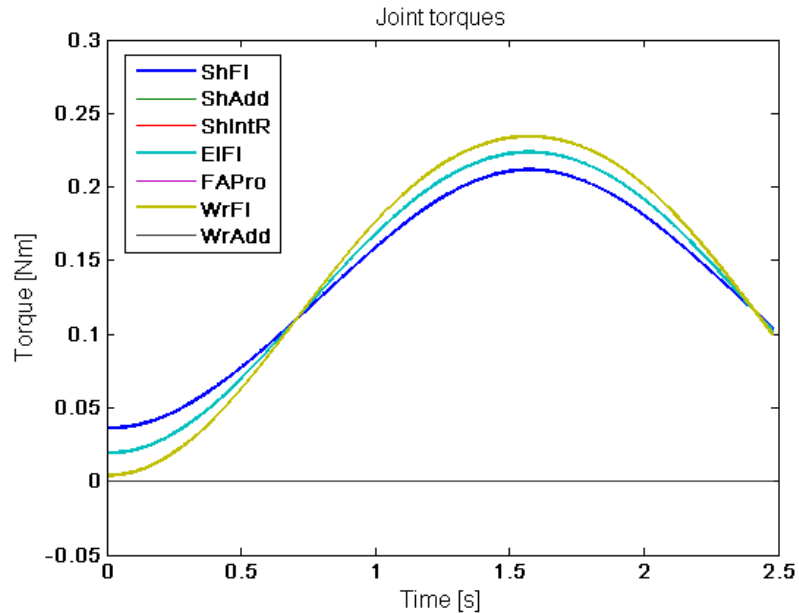


Figure 37: Joint torques for wrist flexion

The first thing to notice in Figure 37 is again the similar shaped torque profiles. As with elbow flexion, the torque for wrist flexion is transferred to the elbow joint and the torque around the elbow is transferred to the shoulder. In Figure 38 movement of joints besides the wrist flexion cannot be seen. The flexion of the wrist involves only one mass, to be tilted in 45 degrees. As the mass of the hand is smaller than the masses of the forearm and the upper arm, there is a lower amplitude (0.013°) of oscillation for shoulder and elbow flexion.

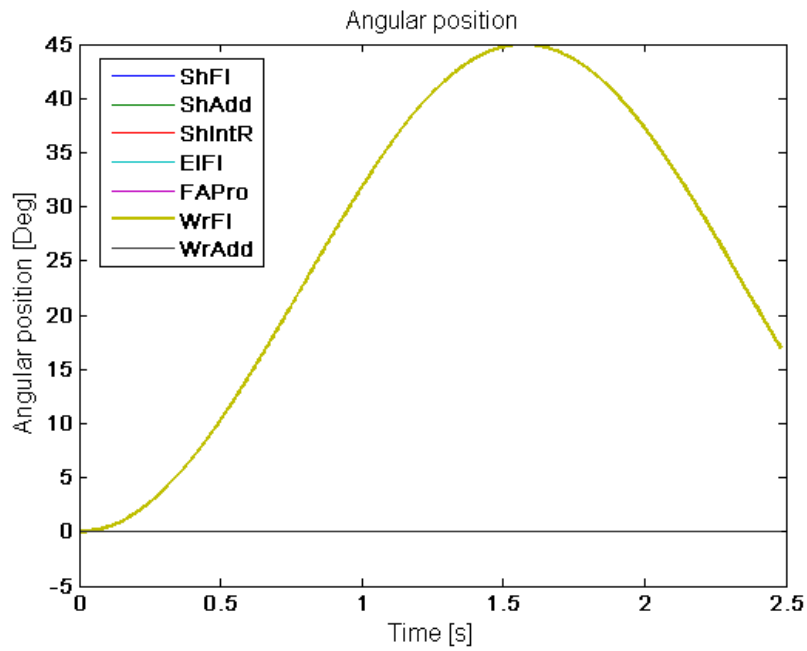


Figure 38: Angular position for wrist flexion

Wrist adduction

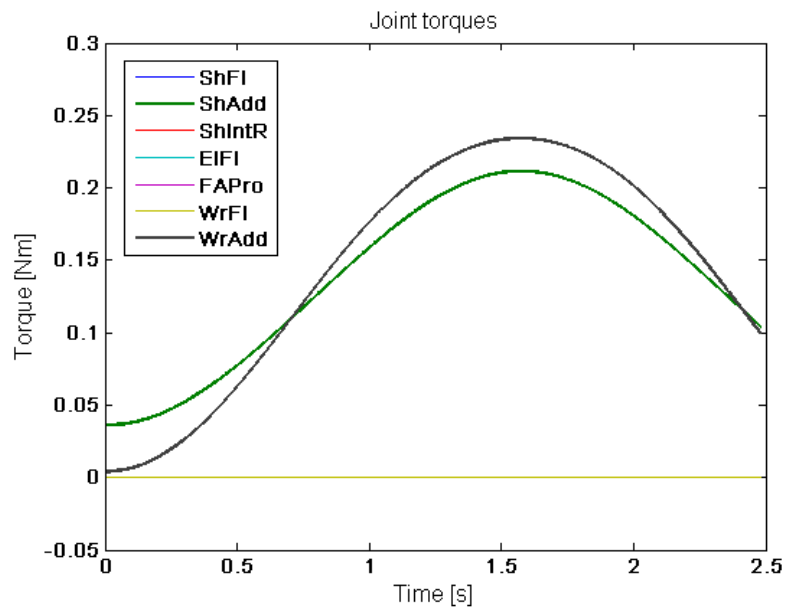


Figure 39: Joint torques for wrist adduction

For wrist adduction torque profiles, Figure 39, the same pattern as for elbow and wrist flexion can be seen. Here again the moment around the wrist is transferred to the proximally located joint with the same working plane. Figure 40 shows the resulting movement and there are no visible oscillation of the other joints as the shoulder adduction oscillates with an amplitude of 0.01 degree.

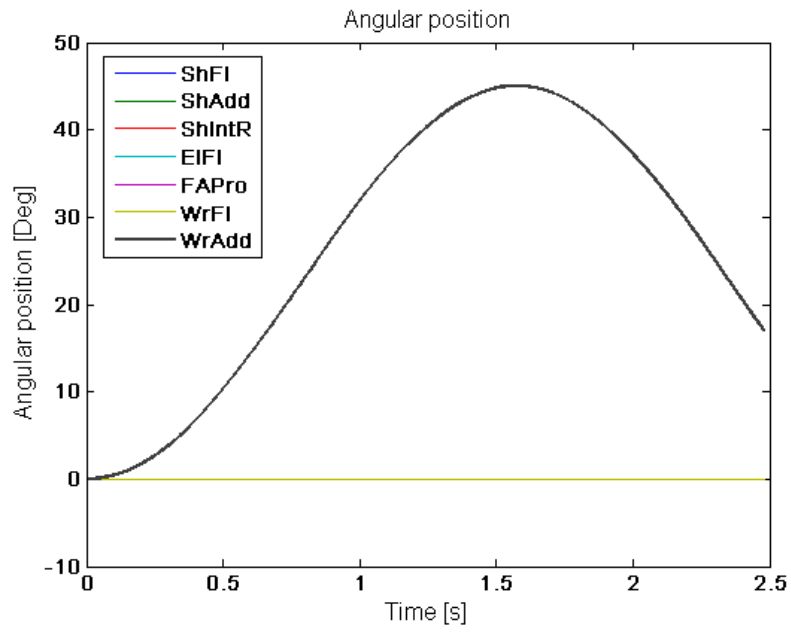


Figure 40: Angular position for wrist adduction

V. Sequence of revolute joints

In section 7.4 the results of the three sequences of revolute joints are discussed for shoulder adduction. This appendix comprises the remaining joint movements. For each single joint actuation, the effect of revolute joint sequence is checked.

Shoulder flexion

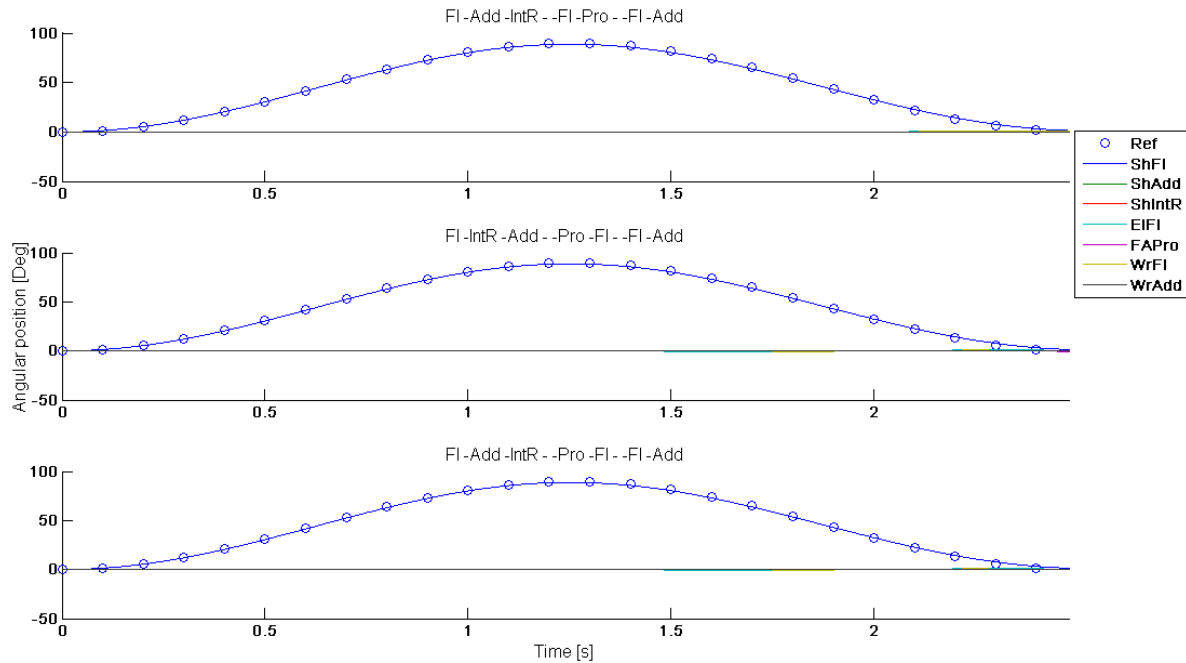


Figure 41: Sequence results shoulder flexion

For shoulder flexion it can be seen in Figure 41 that all sequences do well. However in the original sequence the other joints start moving a little after two seconds, in the other two sequences after 1.5 seconds.

Shoulder internal rotation

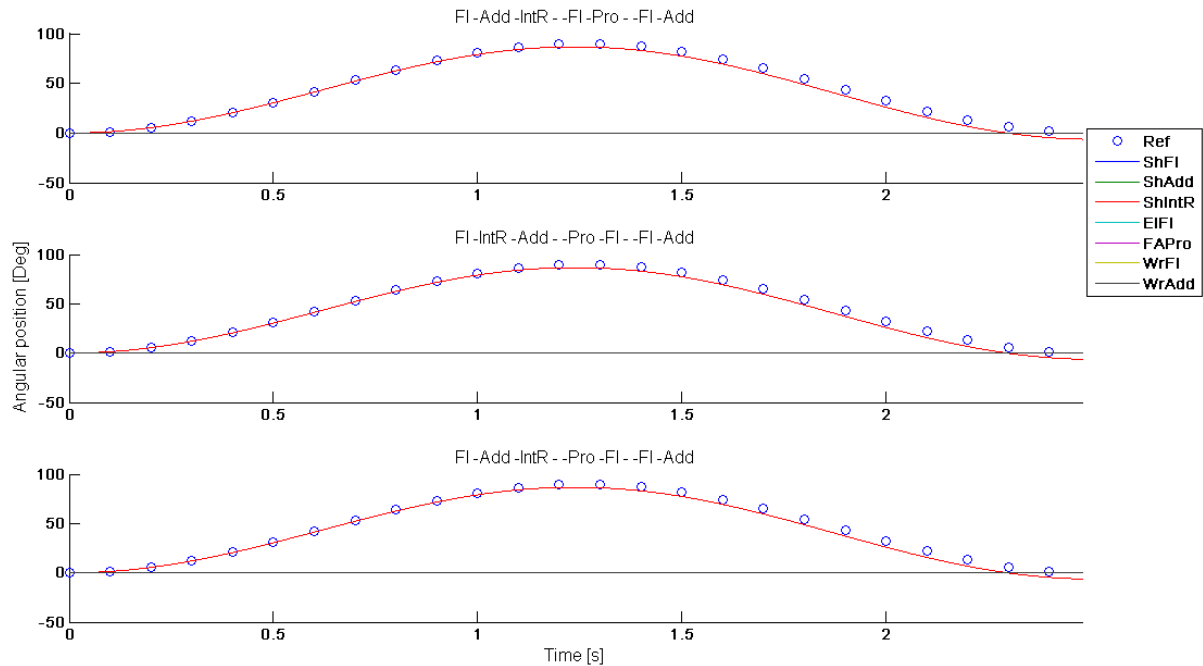


Figure 42: Sequence results shoulder internal rotation

In shoulder internal rotation all sequences show exactly the same behaviour, as can be seen in Figure 42, making it not sensitive to a change in joint sequence.

Elbow flexion

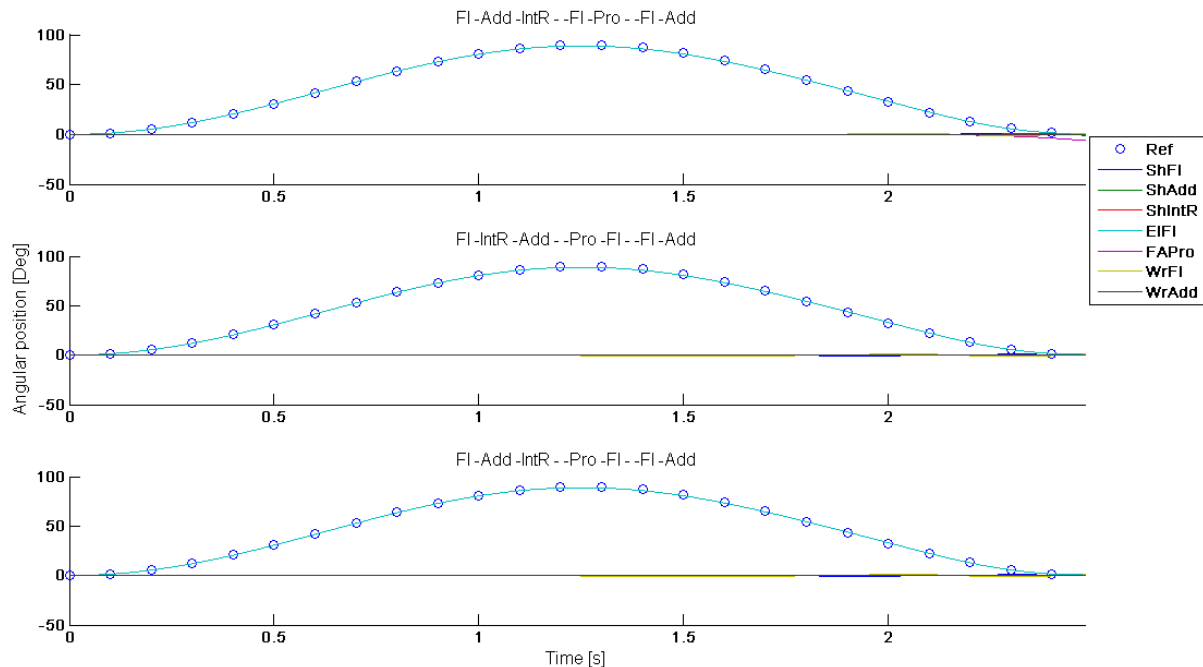


Figure 43: Sequence results elbow flexion

Elbow flexion, Figure 43, shows behaviour similar to shoulder flexion. The original sequence shows movement of the other joints from about two seconds, now with in the end a rather present forearm pronation. The other sequences show a slight movement of the flexion joints at the shoulder and wrist from about 1.2 seconds onward.

Forearm pronation

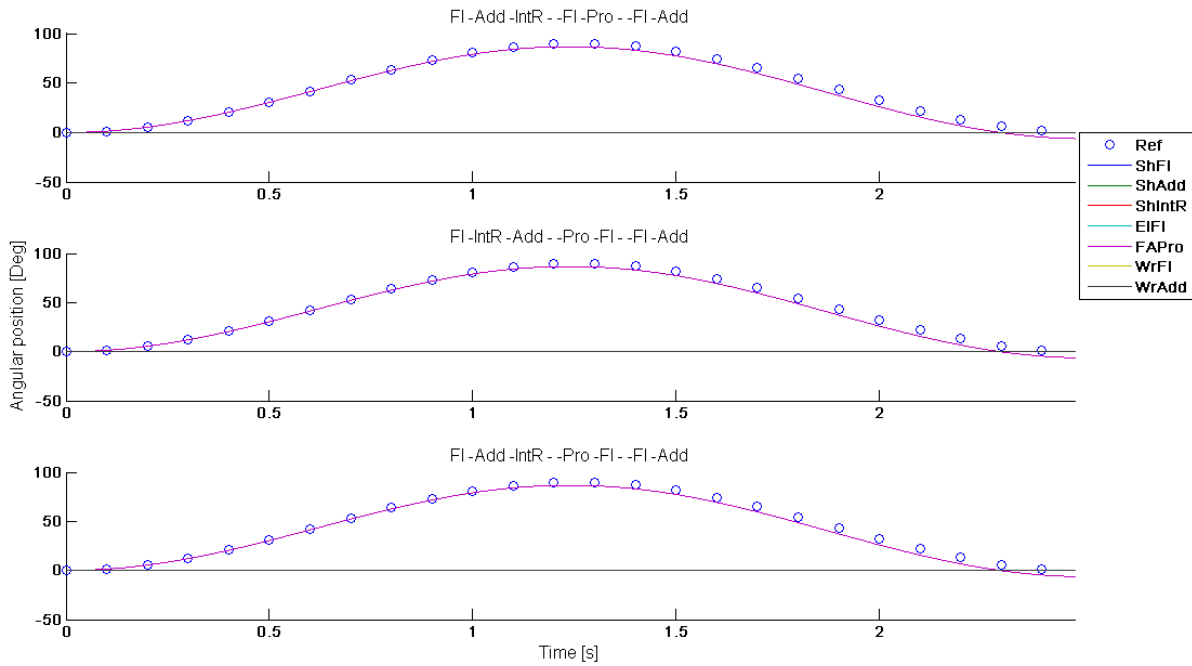


Figure 44: Sequence results forearm pronation

For the rotational degree of freedom, forearm pronation, it can be seen in Figure 44 that it behaves like shoulder internal rotation and thus no difference can be observed between the sequences.

Wrist flexion

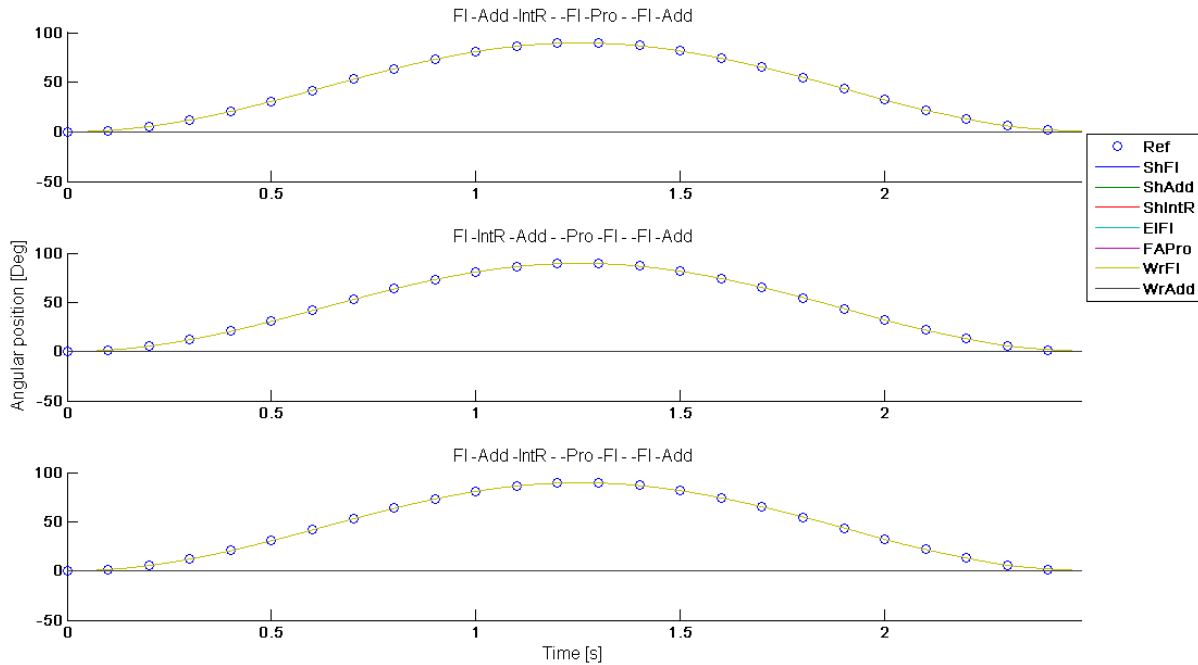


Figure 45: Sequence results wrist flexion

Wrist flexion, shown in Figure 45, shows good behaviour and there is no difference seen for the different joint sequences.

Wrist adduction

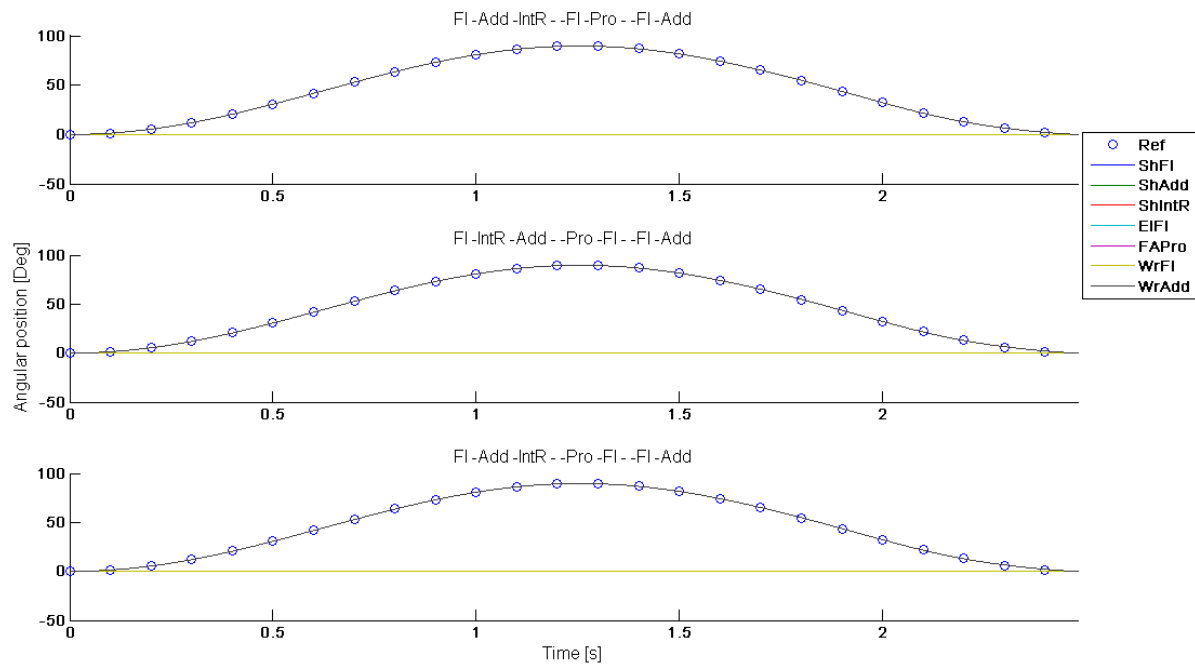


Figure 46: Sequence results wrist adduction

Also wrist adduction depicted in Figure 46 shows equal behaviour for all joint sequences. However for all graphs it should be noted that, apart from the rotational movements, there are slight oscillations occurring with maximum amplitudes of approximately 1.2 degrees for shoulder and elbow flexion movement. For all the sequences the shape of the oscillation is the same but there is a small difference in amplitude.